UNIVERSITY OF CAMBRIDGE
Department of Engineering

# Investigations into steel-glass adhesive joints

Technical Report Number: CUED/D-STRUCT/TR231
Prepared by: Dr M. Overend, Q. Jin and J. Watson
For: The Steel Construction Institute
Date:29 June 2010

# Contents



Prepared by:

Qian Jin
Research Student
Glass & Façade Technology Research Group

James Watson
Research Student
Glass & Façade Technology Research Group

Checked by:

Dr Mauro Overend
Coordinator
Glass & Façade Technology Research Group

## Executive Summary

This report provides information on the structural performance of five candidate adhesives for steel-to-glass connections, based on experimental, numerical and analytical investigations undertaken by the Glass and Façade Technology Research Group at the University of Cambridge. The investigations were limited to small scale tests subjected to short term loading in laboratory conditions and as such do not provide sufficient information for designing or specifying real-world connections.

This report however provides essential information for constructing accurate numerical models of steel-glass adhesive joints and is useful for identifying the most promising adhesives on which further tests should be carried out.

The precise details of the steel-glass connection (and hence its performance requirements) have yet to be established. Nevertheless the report identifies three potentially suitable adhesives that should be investigated further. A quantitative adhesive selection chart is provided in the conclusion that could be used to further reduce the number of potentially suitable adhesives when the performance requirements are established.

The report was commissioned by the Steel Construction Institute and formed part of the "Innoglast" research project funded by the European Commission.

## Acknowledgements

The authors would like to thank the following for their contribution to this study:

- Mr. Sigurd Sitte for the free supply of and technical advice on the Dow Corning adhesive.
- Mr. Peter Collins of Hourglass Ltd. for free supply of and technical advice on the Bohle adhesive
- Mr. Ramoon Ahmed of Holdtite Ltd. for the free supply of and technical advice on the Holdtite adhesive.
- Mr. Geoff Richards of Sika UK Ltd for the free supply of and technical advice on the Sika adhesive.
- Mr. Jean-Philippe Curdy of Potters-Ballottini Ltd. for free supply of and technical advice on the glass microsphere spacers.
- Mr. Phil More at 3M for technical advice on the 3M adhesive.
- Mr. Marco Zaccaria of the Technical University of Bari for his assistance with the testing of the specimens during his stay at Cambridge.

# 1 Introduction

Physical experiments were designed and undertaken to determine the structural performance of a range of adhesives for glass-steel architectural applications when subjected to quasi-static short-term loads. Single-lap shear tests and adapted T-peel tests were carried out on 6 adhesives. The adhesives tested were a two part silicone adhesive Dow Corning DC993 (DC993); a silicone adhesive Dow Corning DC895 (DC895); a two part polyurethane adhesive SikaForce 7550 L15 (SikaForce); a two part acrylic adhesive Holdtite 3295 (Holdtite); a UV cured acrylic adhesive Bohle 682-T (Bohle) and a two part modified epoxy adhesive 3M 2216B/A (3M). The tests were commissioned by the Steel Construction Institute and formed part of the "Innoglast" research project funded by the European Commission.

In parallel, analytical and numerical models were undertaken to predict the performance of the adhesive joints. In order to complete these numerical and analytical investigations it was necessary to undertake preliminary investigations on the adhesives to establish some of the fundamental mechanical properties were not available from the manufacturers / suppliers.

The preliminary investigations on the bulk adhesive properties are described in section 2 and the experimental investigations on the steel-glass specimens are summarised in section 3. Section 4 provides information on the numerical and analytical modelling and the goodness of fit between these models and the experimental data.

# 2 Preliminary Investigations

In order to model the adhesives accurately it was important to determine the effects of stress magnitude and stress duration on the shear modulus of the bulk material. Some of the mechanical properties required to characterise the stiffness of the bulk material were available in the respective adhesive data sheets (Appendix E) and some further properties were provided through subsequent communications with the adhesive manufactures. The information made available by the manufacturers was however insufficient to assemble an accurate constitutive model of the adhesives. In particular, none of the manufacturers could provide sufficient data to decouple the visco-elastic decay constant from the elasto-plastic behaviour of adhesives. Preliminary experiments using dumbbells of each adhesive were therefore conducted to determine the visco-elastic and elasto-plastic properties independently of each other. The visco-elastic properties were first obtained, and a discrete loading strategy was subsequently devised to establish the elasto-plastic properties.

## 2.1 Dumbbell Preparation

The bulk material properties of the adhesives were obtained from tensile tests on adhesive dumbbells shown in Figure 2.1 following the procedures set out in BS EN ISO 527-1:1996 and BS EN ISO 527-2:1996 (BSI, 1996a)

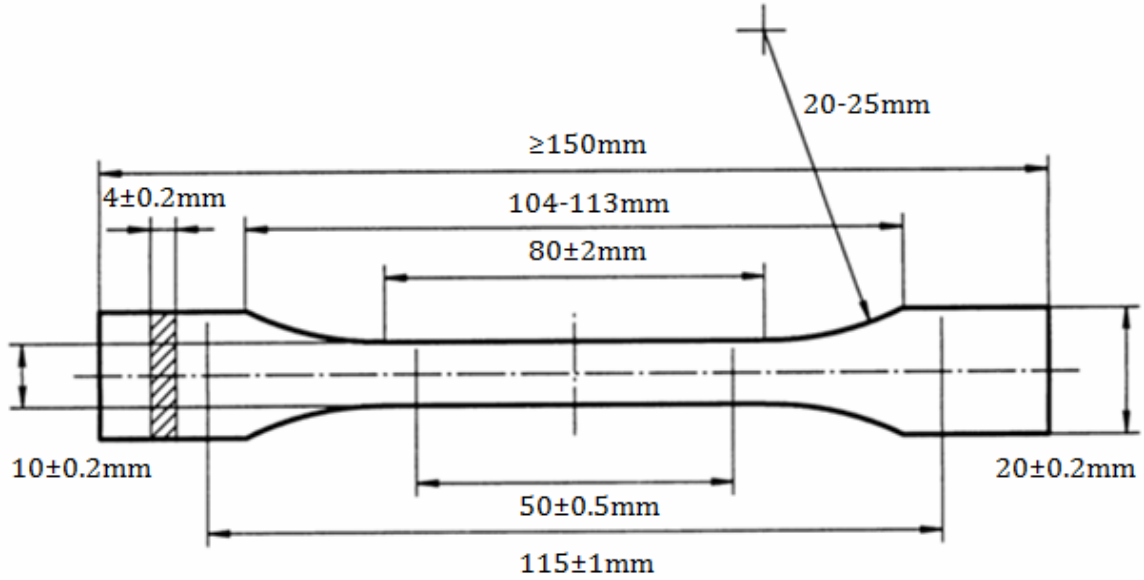


**Figure 2.1** Dumbbell Geometry (BSI, 1996a)

The dumbbells were cast into specially prepared silicone rubber moulds (*cf.* product datasheet, Appendix E) which were in turn cast around existing injection moulded nylon dumbbells. The silicone rubber was out-gassed during curing (using a vacuum chamber) in order to minimise the number of trapped air bubbles, improving the quality of the mould. Once cured, the mould was sprayed with a medium duty silicone release agent and the adhesives were deposited into the mould and out-gassed to remove air bubbles. Finally a sheet of PTFE was manually pressed onto the on top of the mould squeezing out excess adhesive in order to give a good finish on both sides of the dumbbell.

All the dumbbells were 4mm thick apart from the Holdtite and Bohle dumbbells, which were cast into 1mm thick dumbbells. For the Bohle adhesive this constraint was imposed by the depth of penetration of the UV radiation. It is possible to cast a 4mm thick dumbbell using the Holdtite, but the heat generation during, and the brevity of, the curing process results in distortions and entrapped air bubbles in the dumbbell. By reducing the thickness to 1mm, a better sample quality was achieved (some air bubbles were still present as there was not

sufficient time to out-gas the samples before curing took place). A range of the dumbbells produced is shown in Figure 2.2.

**Figure 2.2** Holdtite, Bohle, 3M and DC993 Dumbbells (shown from left to right).

Whilst the preparation of the SikaForce and 3M adhesives was straightforward and high quality dumbbells were produced, there were several issues associated with the other adhesives. The DC993 was very difficult to separate from the mould, even with the release spray. As a result the edge quality of these dumbbells was not as good as the other adhesives. The Bohle was cured in 2/3 layers to ensure that no uncured adhesive was left in the centre of the sample. The Holdtite was difficult to prepare and to ease this; the ratio of the hardener to resin was decreased as much as possible without affecting the tensile strength (as stated in the product datasheet in Appendix E). This afforded us enough time to achieve a level finish on the dumbbell, even if all the air bubbles could not be removed.

## 2.2 Procedure for determining the viscous properties of adhesives

All the numerical modelling was carried out in a commercial Finite Element software LUSAS v14.3. The software describes visco-elasticity by a stress relaxation function:

$$G(t) = G_v e^{-\beta t} \tag{2.1}$$

where $G_v$ is the visco-elastic shear modulus, and $\beta$ is the decay constant. These material properties were not available from the adhesive manufactures and were determined from the tensile tests on adhesive dumbbell described in section 2.1. The tests were carried out on an Instron 5500R electromechanical testing machine.

The ideal experimental procedure fro determining visco-elastic properties is to apply an instantaneous uniform tension to the dumbbells up to a predefined extension, followed by a period of unchanged extension while the decay of the load is recorded. However, in practice viscous energy is dissipated during the time required to achieve the predefined extension, i.e. the fast loading stage. Moreover, due to the momentum generated by a fast loading rate, the extension tends to overshoot the predefined extension, and then returns to it, which leads to a further loss of viscosity. Therefore, a correction of the experimental data was required and is described here using the 3M adhesive dumbbell test as an example (Figure 2.3). Assuming that in the very early loading stage (confined by a change in the stress / time gradient of less than 20%) no viscosity is lost, the slope in that stage is assumed to be purely elastic and is extrapolated to determine the viscosity-independent stress (point *A* in Figure 2.3). This corresponds to the time when the predefined extension is first reached (point *A* in

Figure 2.4). From Figure 2.4 it is possible to determine the time at which constant extension is reached, denoted as point *B*. The corrected visco-elastic behaviour, shown as dashed lines in Figure 2.3 and Figure 2.4, are therefore obtained by joining the origin with point *A* through to point *B*. A small error is introduced by joining point *A* and point *B* with a straight line, but given the relatively long time-scale of the test (*cf.* Figure 2.5) this error is considered to be negligible.

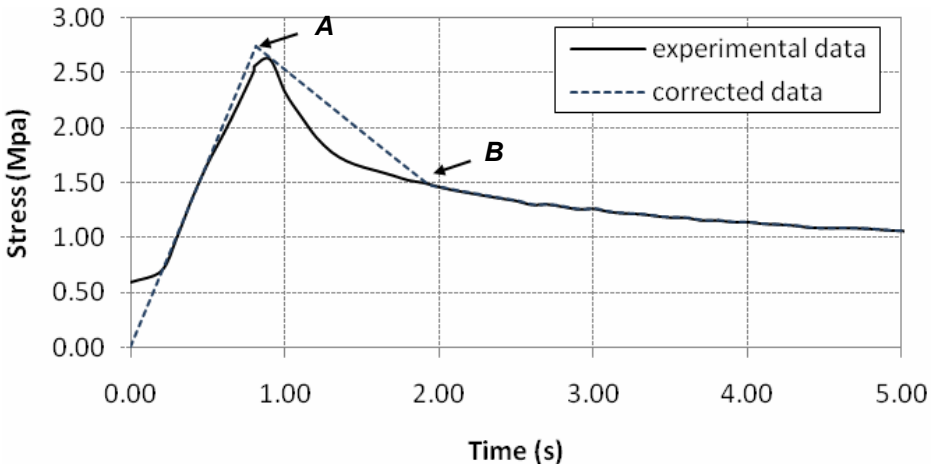


**Figure 2.3** Extract of stress *vs.* time relationship from visco-elasticity test of 3M dumbbell

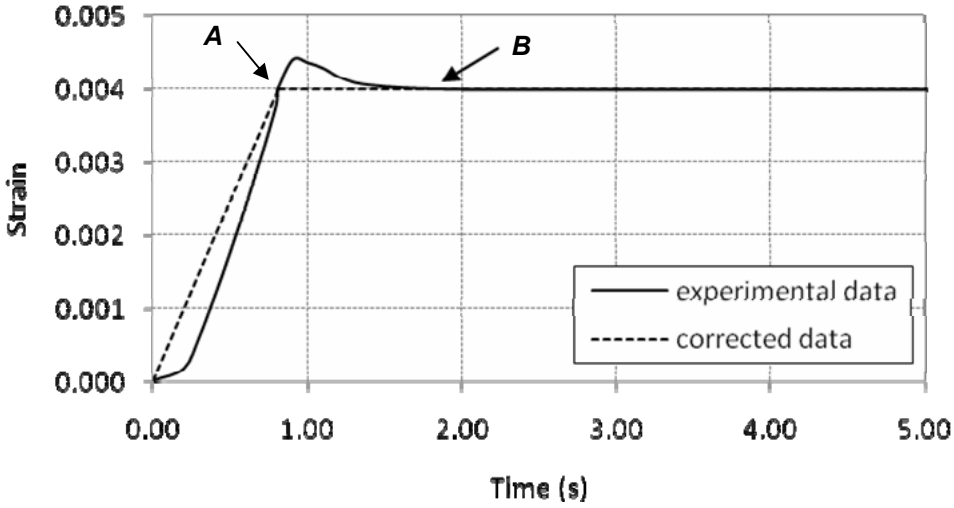


**Figure 2.4** Extract of strain *vs.* time relationship from visco-elasticity test of 3M dumbbell

Since the extension and Poisson's ratio are known, the stress *vs.* time relationship can be converted into shear modulus *vs.* time relationship, from which the decay constant $\beta$ can be obtained by curve fitting and the shear modulus $G_v$ can be calculated by subtracting the residual shear modulus from the initial shear modulus, as shown in Figure 2.6.

Two methods have been used to identify the appropriate decay constant. Method 1 (M1) minimises the sum of the square of differences between the experimental value for shear modulus and those calculated from the stress relaxation function (Eq 2.1), which produces a decay constant of 0.39 (denoted by the dashed line in Figure 2.6). This method is preferable if the shear modulus is of major concern, but it will underestimate the adhesive stiffness during the decay period. Method 2 (M2) minimises the sum of square of differences between time from the test and that from the stress relaxation function (Eq 2.1), which produces a decay constant of 0.040 (denoted by the dotted line in Figure 2.6). This method is preferable

if the total decay time is of major concern, but will lead to an overestimation of the adhesive stiffness at high strain rates. In this investigation, the strain rates are relatively low and the shear modulus is of primary interest, therefore method 1 is preferred. Furthermore, this produces more conservative results for real world applications of the data. Nevertheless, results from both methods (M1 and M2) were plotted in subsequent parts of this report to define an upper and a lower limit within which the experimental results are expected to lie. The visco-elastic properties of all the adhesives obtained by both methods are summarised in Table 2.1.

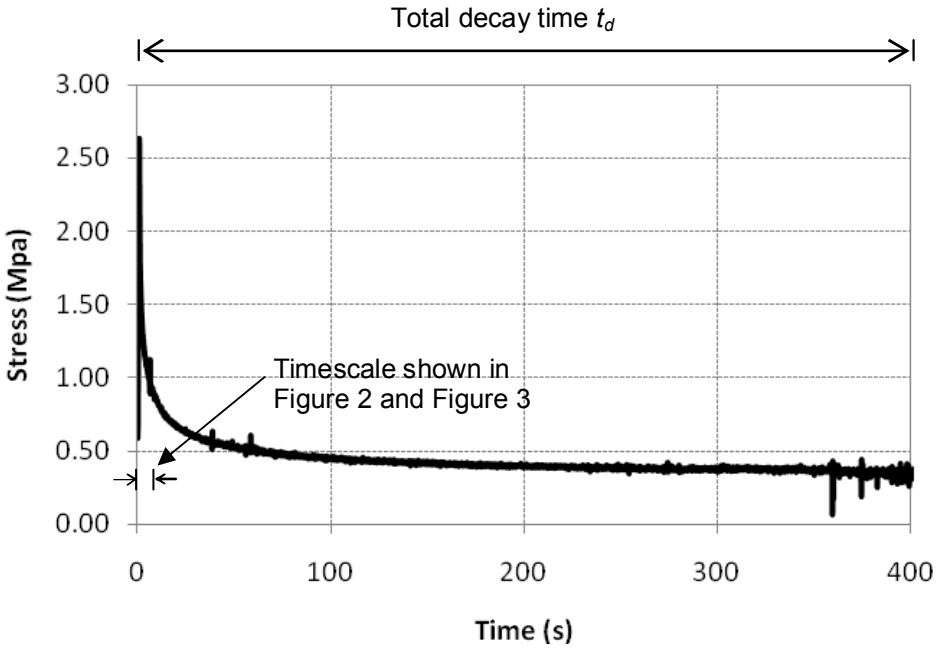


**Figure 2.5** Complete stress *vs.* time relationship for 3M dumbbell test

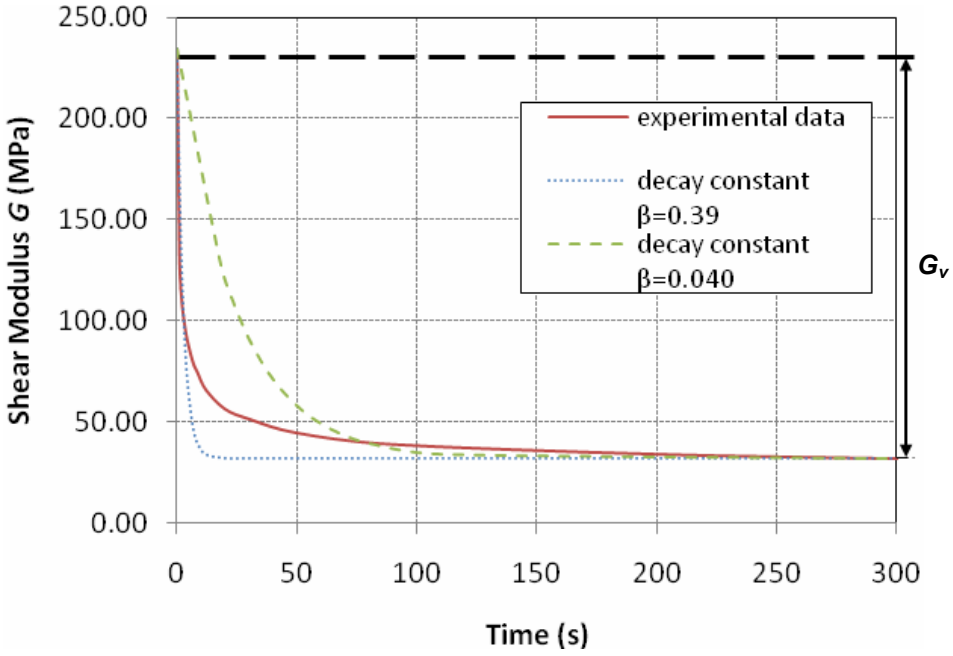


**Figure 2.6** Shear modulus *vs.* time relationship for 3M dumbbell

**Table 2.1** Viscc-elastic properties of adhesives.

| | | DC993 | SikaForce* | Holdtite | 3M | Bohle |
|---|---|---|---|---|---|---|
| **Poisson's Ratio** | | 0.49 | 0.39 | 0.39 | 0.46 | 0.30 |
| **$G_v$ (MPa)** | | 0.031 | 1.50 | 195.89 | 201.88 | 386.23 |
| **$t_d$ (s)** | | 54 | 92 | 600 | 500 | 1000 |
| **$\beta$** | **M1** | 1.23 | 0.77 | 0.087 | 0.39 | 0.022 |
| | **M2** | 1.30 | 0.75 | 0.075 | 0.040 | 0.0069 |

** SikaForce properties were obtained from reused samples.*

## 2.3 Procedure for determining the elasto-plastic properties of adhesives

The total decay time, $t_d$, taken for the shear modulus to fall to the residual (constant) value, was identified from the viscous test described in the previous section. The elasto-plastic properties were tested experimentally using a discrete load-step strategy on dumbbell specimens of the adhesive in an Instron 5500R electromechanical testing machine. The total loading period was divided into at least 10 intervals, and in each increment the load was kept constant for a duration $t_i = t_d$. The last points of each load interval, referred to as the stabilised points in Figure 2.7, therefore represent load *vs.* displacement relationship of the adhesive independent of viscous decay. An expression for the elasto-plastic stress-strain relationship was obtained by polynomial curve fitting to these stabilised points (Figure 2.8). The failure stress was obtained by substituting the mean failure strain of the nominally identical dumbbells tested into the polynomial function (Figure 2.8). The elasto-plastic properties for each adhesive are summarised in Table 2.

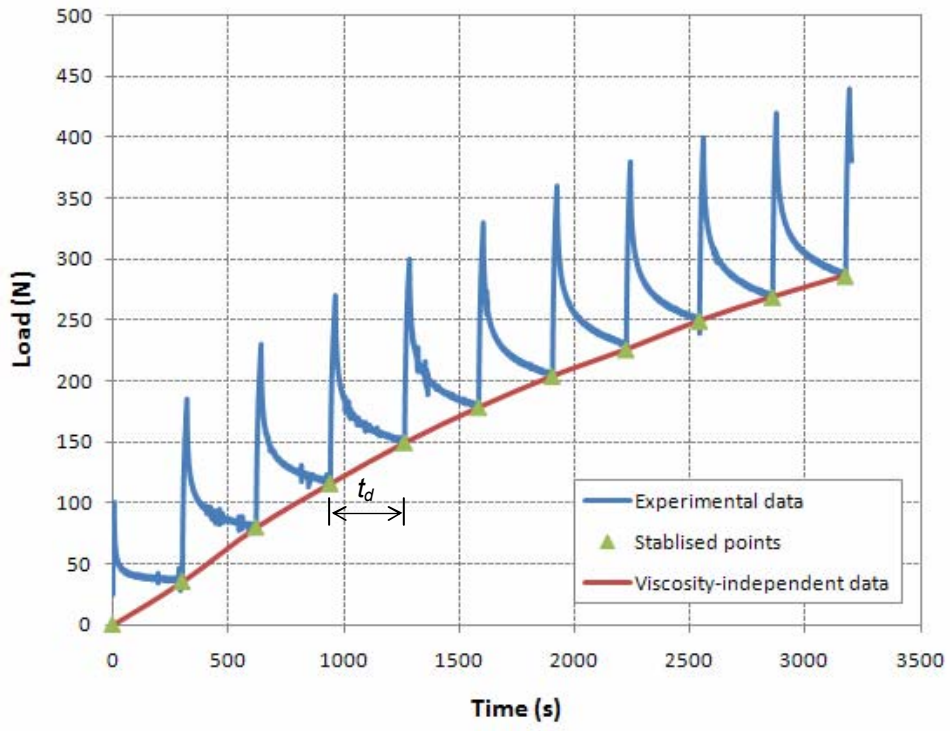


**Figure 2.7** Typical load *vs.* displacement curve for elasto-plastic test on 3M dumbbell

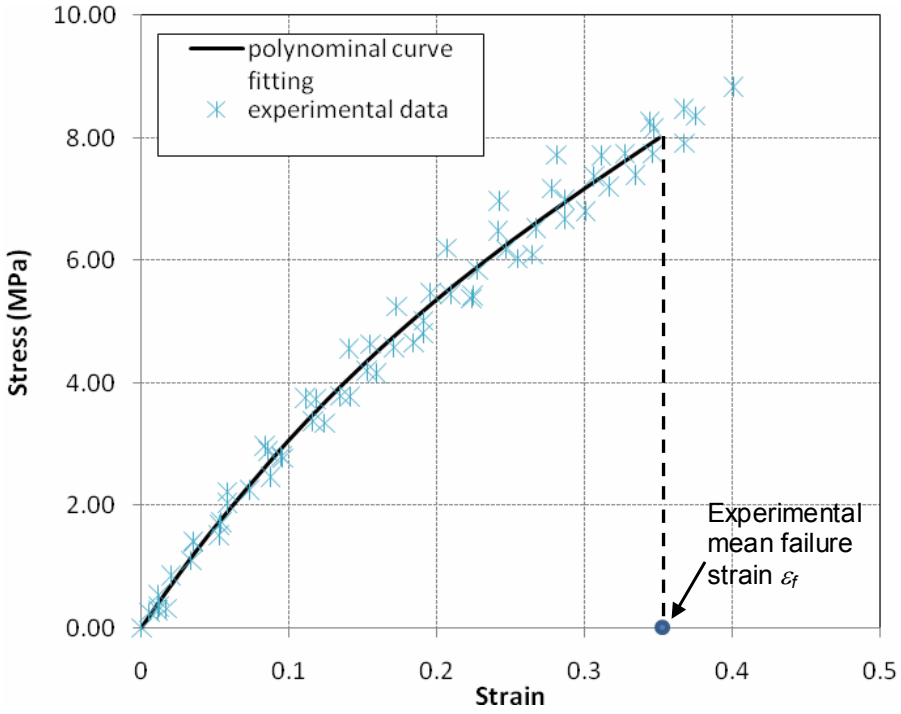


**Figure 2.8** Experimental data and polynomial curve fitting curve for the stress *vs.* strain relationship of 3M.

**Table 2.2** Summary of stress *vs.* strain relationship independent of viscosity.

| | Elasto-plastic stress-strain relationship | $R^2$-value | Failure strain $\varepsilon_f$ |
|---|---|---|---|
| **DC993** | $\sigma = 0.311\varepsilon^3 - 1.0691\varepsilon^2 + 1.8825\varepsilon$ | 0.9943 | 1.33 |
| **Holdtite** | $\sigma = 1142.312\varepsilon$, for $0 \le \varepsilon \le 0.00135$; $\sigma = 227681\varepsilon^3 - 13587\varepsilon^2 + 324.95\varepsilon + 1.1255$, for $\varepsilon > 0.00135$ | 0.9132 | 0.0265 |
| **3M** | $\sigma = 49.037\varepsilon^3 - 53.513\varepsilon^2 + 35.575\varepsilon$ | 0.9858 | 0.35 |
| **Bohle** | $\sigma = -2336.4\varepsilon^3 - 705.81\varepsilon^2 + 53.499\varepsilon$ | 0.9196 | 0.038 |
| **SikaForce*** | $\sigma = -9.2036\varepsilon^4 + 20.985\varepsilon^3 - 18.455\varepsilon^2 + 10.23\varepsilon$ | 0.9997 | 1.06 |

** SikaForce was tested using a different loading strategy, i.e., continuously slow loading, which means that this stress vs strain relationship is not completely viscosity-free. Due to lack of materials, further investigation was not possible.*

**Conclusions**

Establishing the fundamental bulk material properties of adhesives is a non-trivial task, but is essential for constructing accurate numerical and analytical models. The visco-elastic elastic properties may become negligible for long load durations, but may be significant for load durations that are relevant to this steel-glass connection such as soft body impact, hard body impact and wind induced loads. Ignoring the viscous characteristics of the adhesive behaviour would result in an overestimation of the deformation and an underestimation of the stresses.

The two methods used to identify the appropriate decay constant (i.e. M1 and M2) produce comparable $\beta$ values for DC993, SikaForce, and Holdtite, while significantly different values for 3M and Bohle. These discrepancies suggest that the visco-elastic relationship in Equation 2.1 can accurately characterise the performance of some but not all adhesives. This is an interesting phenomenon that merits further research, but is outside the scope of this investigation.

The adhesive properties shown in table 2.1 that the adhesives investigated in this study have a very wide range of shear moduli and decay times. For example the stiffest adhesive is 12,500 stiffer than the most flexible adhesive. Furthermore, despite their different chemical compositions, the elastic shear moduli, $G_v$, of the different adhesives seem to be related to the bond thickness, t, such that $G_v \propto e^{-t}$.

# 3 Experimental Investigations

The ability of the six adhesives (DC993, DC895, SikaForce 7550, Holdtite 3295, and Bohle 682-T) to form a load bearing steel-to-glass connection was tested experimentally through a single lap shear (SLS) set-up based on ASTM D1002-99 (ASTM, 1999) and a T-peel test adapted from the guidelines in ASTM D1876-93 (ASTM, 1993)..The test geometries used are shown in Appendix A – Test Geometries. A total of sixty specimens were tested composed of 5 specimens x 6 adhesives x 2 test set-ups.

The two test set-ups (SLS and T-Peel) were designed to give the same bonding area dimensions of 1250mm$^2$, so that a direct comparison could be made between both sets of results. 10mm thick fully toughened glass was used throughout with 150mm x 200mm for the SLS and 150mm x 150mm for the T-Peel.

## 3.1 Sample Preparation

At all times the adhesive manufacturer's recommendations were strictly followed to achieve maximum possible strength. The samples were made up of 2 identical bright mild steel (conforming to BS EN 10277-2:2008) (BSI 2008)) elements and 1 larger fully toughened glass component manufactured to BS EN 12150-2:2004 (BSI 2004).

### 3.1.1 Surface Roughness

Surface roughness of the steel adherends was not a major consideration for some of the adhesives as they have gap filling properties. However, careful preparation of surfaces was required for the adhesives with more stringent guidelines for bond thickness. This applied to Bohle, Holdtite and 3M. Full details are in Appendix D – Extended Sample Preparation. No roughening was applied to the glass surfaces.

### 3.1.2 Cleaning & Priming

For all adhesives, surfaces were required to be free from foreign matter and contaminants such as grease/dust. Dow Corning R40 universal cleaning agent was poured onto a lint free cloth and then wiped over the surfaces and left to evaporate, as per manufacturer recommendations. In addition to this, a primer was required for SikaForce and DC993 (but no primer was required for the other adhesives). More details are in.

### 3.1.3 Sample Assembly

Specially designed jigs were used to ensure that the joints were aligned correctly. The optimal thickness of the adhesives varied considerably from 6mm for DC993 to 0.106mm for Bohle. Glass microsphere spacers were used to ensure optimal spacing in thin adhesive layers. Thicker adhesive layers were achieved by using temporary glass shims to produce the required bond line thickness. The thickness of each joint is specified in Table 3.1. Joint movement during curing was kept to a minimum to prevent imperfections such as air bubbles entering the joint. The Bohle adhesive required UV radiation to cure. Full details of the experimental preparation and bond widths are attached in Appendix D.

**Table 3.1** Summary of Preparation Values for each Adhesive

| | ***DC993*** | ***DC895*** | ***SikaForce*** | ***Holdtite*** | ***3M*** | ***Bohle*** |
|---|---|---|---|---|---|---|
| **Handling Time** | 24 hrs | 24hrs | 1 hr | 2-3 mins | 8-12 hrs | 40s |
| **Curing Time** | 7 days | 7 days | 2-3 hrs | 5 mins | 7 days | 40s |
| **Surface Roughness** | N/A | N/A | N/A | $R_a$ 0.47µm<br>$R_q$ 0.66µm | $R_a$ 0.47µm<br>$R_q$ 0.66µm | $R_a$ 0.2µm<br>$R_q$ 0.3µm |
| **Bond Thick. (mm)** | 6 | 6 | 3 | 0.106 | 0.212 | 0.106 |
| **Displacement Rate (mm/min)** | 2 SLS<br>2 TPeel | 6 SLS<br>6 TPeel | 2 SLS<br>1 TPeel | 0.18 SLS<br>0.1 TPeel | 0.1 SLS<br>0.1 TPeel | 0.1 SLS<br>0.1 TPeel |

## 3.2 Test Apparatus

Tests were performed using an Instron 5500R electromechanical testing machine. Load and both in-plane and lateral displacements were measured by means of linear variable differential transformers (LVDTs). The apparatus for both of the test set-ups are shown in Figure 3.1.

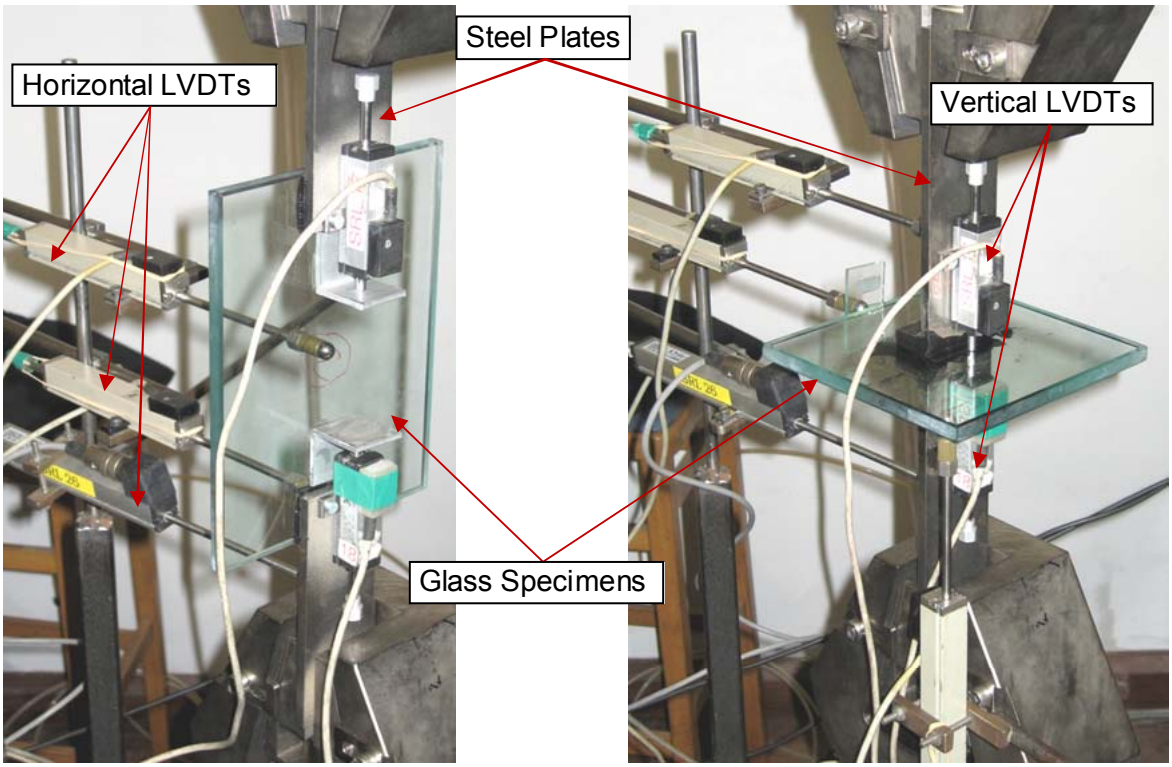


**Figure 3.1** Test Setup for both the Single Lap Shear (left) and T-Peel (right) tests

## 3.3 Test Procedure

Due to the elasto-plastic nature of adhesive failure the tests were all displacement controlled rather than load controlled. The tests were manually halted once the load had fallen to zero and total failure had occurred.

The visco-elastic behaviour of adhesives means that the displacement rate for these tests is an important consideration. Different strain rates would produce different responses and hence results. Individual displacement rates for each adhesive were chosen to induce failure within 5 to 10 minutes. The displacement rates are shown in Table 3.1.

## 3.4 Test Results & Observations

### 3.4.1 Results

A summary of the results is shown in Table 3.2. The coefficient of variation (= standard deviation / mean) is a dimensionless measure of the dispersion of the maximum loads and allows comparisons of the variability of the different adhesives tested.

The load-extension results for each adhesive are plotted in Appendix B.

**Table 3.2** Summary of Test Results (* Denotes Glass Failure)

| *Adhesive* | *Test Type* | *Max Load (kN)* | *Extension at Max Load (mm)* | *Time to Max Load (s)* | *Coefficient of Variation* |
|---|---|---|---|---|---|
| **DC895** | SLS | 1.205 | 23.39 | 461 | 0.259 |
| | | 0.580 | 15.76 | 256 | |
| | | 0.786 | 19.93 | 345 | |
| | | 0.955 | 20.53 | 382 | |
| | | 0.916 | 18.94 | 364 | |
| | T-Peel | 1.001 | 11.79 | 282 | 0.241 |
| | | 0.788 | 12.17 | 208 | |
| | | 0.649 | 8.48 | 180 | |
| | | 1.139 | 15.70 | 210 | |
| | | 1.185 | 9.69 | 190 | |
| **DC993** | SLS | 0.853 | 8.66 | 475 | 0.065 |
| | | 0.845 | 7.31 | 465 | |
| | | 0.772 | 8.60 | 460 | |
| | | 0.733 | 7.34 | 366 | |
| | | 0.774 | 7.23 | 398 | |
| | T-Peel | 1.369 | 2.71 | 125 | 0.105 |
| | | 1.498 | 3.75 | 132 | |
| | | 1.353 | 2.21 | 110 | |
| | | 1.431 | 2.16 | 98 | |
| | | 1.129 | 1.42 | 81 | |
| **SikaForce** | SLS | 1.865 | 1.76 | 99 | 0.484 |
| | | 1.863 | 2.91 | 229 | |
| | | 0.554 | 1.35 | 86 | |
| | | 1.675 | 1.38 | 151 | |
| | | 0.717 | 1.65 | 103 | |
| | T-Peel | 1.025 | 0.90 | 43 | 0.205 |
| | | 1.208 | 0.31 | 25 | |
| | | 1.486 | 0.26 | 26 | |
| | | 1.526 | 0.41 | 40 | |
| | | 0.977 | 0.19 | 15 | |
| **3M** | SLS | 8.389 | 0.21 | 365 | 0.094 |
| | | 9.656 | 0.31 | 418 | |
| | | 9.967 | 0.31 | 364 | |
| | | 7.934 | 0.30 | 302 | |
| | | 9.147 | 0.28 | 330 | |
| | T-Peel | 2.146 | 0.12 | 134 | 0.413 |
| | | 6.226 | 0.18 | 116 | |
| | | 6.093 | 0.05 | 153 | |
| | | 2.951 | 0.13 | 138 | |
| | | 5.227 | 0.06 | 207 | |
| **Holdtite** | SLS | 19.058* | N/A | N/A | 0.081 |
| | | 17.116* | 0.59 | 392 | |
| | | 19.832* | 0.69 | 452 | |
| | | 20.742* | 0.76 | 501 | |
| | | 18.865 | 0.71 | 467 | |
| | T-Peel | 9.727 | N/A | 374 | 0.069 |
| | | 9.867 | 0.64 | 458 | |
| | | 10.007 | 0.60 | 238 | |
| | | 8.381 | N/A | 207 | |
| | | 9.440 | 0.57 | 233 | |
| **Bohle** | SLS | 11.045* | 0.06 | 619 | 0.396 |
| | | 20.382* | 0.15 | 1291 | |
| | | 17.921 | 0.18 | 988 | |
| | | 8.341* | 0.04 | 465 | |
| | | 9.721* | 0.05 | 511 | |
| | T-Peel | 5.169 | 0.07 | 288 | 0.077 |
| | | 15.094 | 0.06 | 674 | |
| | | 13.977 | 0.07 | 644 | |
| | | 16.244 | 0.06 | 726 | |
| | | 16.600 | 0.06 | 778 | |

### 3.4.2 Failure Mechanisms & Observations

When securing the samples in the test machine it was noted that some load was being applied to the samples during the tightening of the jaws. This is largely unavoidable and is most visible in Graph B7, Graph B11 and Graph B12 (the more flexible adhesives dissipated the load through visco-elasticity before readings were taken).

The preferred failure for adhesives involves the adhesive itself failing within the bond thickness. This is known as cohesion failure. This occurred with DC993 and the DC895 for both test geometries (see Appendix C – Images of ). Conversely, the least desirable failure mechanism is adhesion failure, where the adhesive pulls away cleanly from either substrate. This occurred for the SikaForce for both SLS and T-Peel tests (see Appendix C – Images of ), although in some the SiakForce SLS tests recorded a significantly higher load bearing capacity and which corresponded with a partly cohesive failure. Most of the 3M SLS samples failed in cohesion, whereas the 3M T-Peel samples all failed in adhesion with the steel.

The Bohle and Holdtite adhesives performed very differently to the rest of the adhesives. The T-Peel samples performed as expected, with cohesive failure in the adhesive (see Appendix C – Images of ). However glass failure was observed in four of the five SLS samples, with an origin of failure close to the edge of the adhesive joint (see Appendix C – Images of ). Only one out of the five SLS samples failed in cohesion failure for each of these adhesives (17.92kN – Bohle and 18.86kN – Holdtite).

# 4 Analytical and Numerical Investigations

## 4.1 Review of Analytical Methods

Due to the expected complexity (transient, geometrical nonlinearity, material nonlinearity) of the numerical analysis it was decided that a method for validating the output from the finite element model (aside from a comparison with the experimental results) would be useful. An analytical method would also be useful for sizing of future steel-glass adhesive joints. Hence a review of existing literature on the stress concentrations in adhesive joints was carried out.

A quick review of the literature yielded several results. First, the geometry most commonly considered in the literature is a single lap joint and most of the papers review symmetric lap joints i.e. adherends of the same thickness and material. Secondly, the problem is far more complex than initially realised and most analyses make simplifications to eliminate some parameters. Finally, nearly all the work found uses computational methods rather than providing empirical equations that can be used as a quick check. A good overview of the development of stress analysis in single lap joints is described by Adams (Adams, 2005).

However, there is some research that provides equations to approximate the stress distribution in the adhesive layer Her (Her, 1999) and Tsai *et al.* (Tsai *et al.,* 1998) and the former also provides equations for the stress distribution in the adherends as well. These equations are valid for any adherend thickness/material as well as adhesive thickness.

However, the above methods ignore bending which is perhaps a simplification too far. Yet, there are some more complete works which describe analytical formulations that can be implemented using a spreadsheet. One such example is the analysis carried out Bigwood and Crocombe (Bigwood and Crocombe, 1989) which gives the shear and peel stresses in the adhesive. A drawback of this method is that the loading conditions at the ends of the overlap region are required. This is not straight forward as it requires knowledge of the deflections of the adherends and in general loading conditions are only known at the ends of the adherends. A comparison of these techniques with the experimental results is shown in Figure 4.4.

## 4.2 Description of FE models

### 4.2.1 Element type

A 2-D FE model was constructed for each test type using LUSAS v14.3. Since the adhesive width (50.8mm) of the sample was relatively large compared to the adhesive thickness (0.106mm-6mm), deformation in the width direction was considered to be negligible. A quadrilateral quadratic 8-node plane strain element (QPN8) was therefore chosen for both the single-lap and the T-peel connections as shown in Figure 4.1 (LUSAS, 2008). This element is capable of capturing the elasto-lastic and visco-elastic properties of the adhesive. The analysis was performed on a Windows-based PC with a 2.83 GHz processor and 7.93GB of RAM.

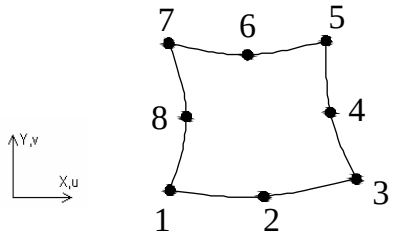


**Figure 4.1** Plane strain element QPN8 (LUSAS, 2008)

### 4.2.2 Boundary Conditions

Half of each connection was modelled due to symmetry. The FE models of the single-lap shear and T-peel connections for the DC993 are shown in Figure 4.2 and Figure 4.3 respectively and are typical of the models used for the other adhesives. The boundary conditions are specified as follows: the experimental assemblies for both the SLS and the T-Peel are symmetric about line *AB* in the *yz* plane therefore $\delta_x$ *and* $M_z$ are restrained along *AB. The experiential* assemblies are also clamped by the testing jaws for 50mmm along the steel plate (indicated as line CD and line EF in Figure 4.2 and Figure 4.3) therefore $\delta_y$, *and* $M_z$ are restrained along *CD and DE.*

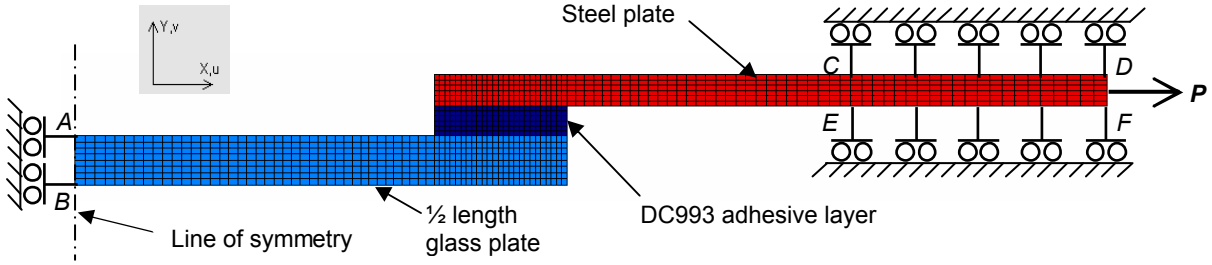


**Figure 4.2** FE model for DC993 SLS connection (boundary conditions and load shown schematically)

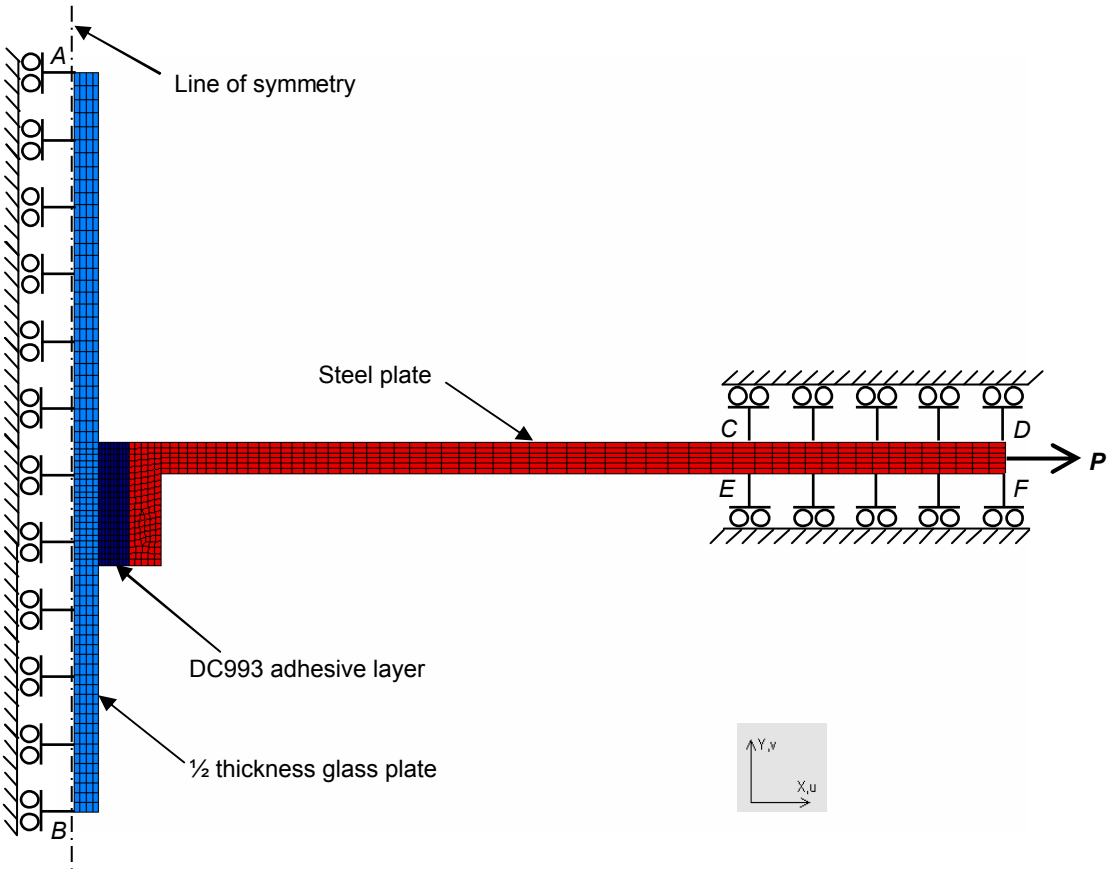


**Figure 4.3** FE model for DC993 T-peel connection (boundary conditions and load shown schematically)

### 4.2.3 Material Properties

Visco-elastic and elasto-plastic and properties of the adhesives were obtained from Table 2.1 and Table 2.2, respectively. The steel plate and glass plate are assumed to be linear perfectly elastic with properties listed in Table 4.1:

**Table 4.1** Material properties of steel and glass

| | Young's Modulus (MPa) | Poisson's Ratio |
|---|---|---|
| **Steel** | 209000 | 0.3 |
| **Glass** | 70000 | 0.22 |

### 4.2.4 Mesh density

The stiffness of the adhesives is very low compared to that of glass and steel, with most of the deformation expected to occur in the adhesives. The convergence test was therefore performed on a 3M SLS specimen by h-refinement. i.e.varying the mesh density uniformly in the adhesive layer. A very coarse mesh was surprisingly accurate. For example a mesh density of 400 elements (4×100 i.e. 4 elements across the thickness of the adhesive layer and 100 elements along the overlap length) produces very similar results to a mesh density of 100 elements (1×100), with the exception of the stress concentrations at the edge of the

adhesive that appear to be underestimated by coarse mesh density (Figure 4.4). This discrepancy is expected to have a negligible effect on the overall structural performance of the adhesive as the elements subjected to a high stress concentration (observed in the 400 elements model in Figure 4.4) will deform plastically and thereby redistribute the elastic energy to the adjacent elements, in doing so the shear stress distribution along the adhesive length will therefore reverts to the 100 elements (Figure 4.4).The elastic strain energy stored in the stress concentration zone represented by the area under the spike in Figure 4.4 is small when compared to the elastic strain energy along the entire adhesive the effect on the total load *vs*. displacement relationship is negligible. This discrepancy between mesh densities will however be significant when determining the stresses imposed on the glass particularly at low loads.

On this basis relatively dense meshes (Table 4.2) were used for each connection which did not have a significant impact on computational time. The adhesive thickness was modelled using 4-6 elements layers, and an appropriate number of elements along the adhesive overlap length were selected to keep the aspect ratio of each element below 10.

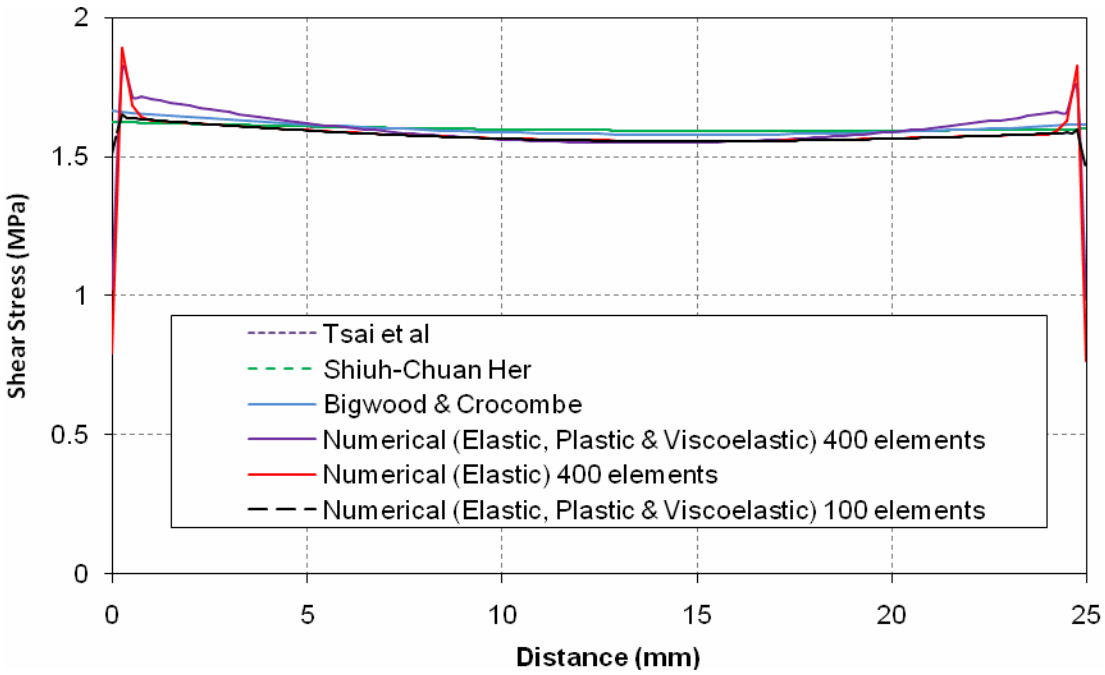


**Figure 4.4** Analytical and numerical shear stresses at mid-depth of the 3M SLS adhesive joint (*P* = 2kN)

**Table 4.2** Mesh density of the adhesive layer

| | | ***DC993*** | ***SikaForce*** | ***Holdtite*** | ***3M*** | ***Bohle*** |
|---|---|---|---|---|---|---|
| **No. of Elements** | SLS | 6 × 25 | 6 × 25 | 4 × 200 | 4 × 100 | 4 × 200 |
| | T-peel | 6 × 20 | 6 × 20 | 4 × 200 | 4 × 100 | 4 × 200 |

The differences between the numerical solutions (elastic and visco-elasto-plastic) and the analytical solutions (which adopt an elastic material model) shown in Figure 4.4 were explored further by plotting the shear stress distribution for the 3M SLS joint at different loads Appendix G). A brief interpretation of these results is provided in section 4.3.1.

### 4.2.5 Loading

The loading *P* is applied as a displacement rate (i.e. a velocity in mm/s) at the end of the steel plate, corresponding to Line DF in Figure 4.2 and Figure 4.3. The displacement rate for each adhesive corresponds to the experimental displacement rate shown in Table 3.1

### 4.2.6 Non-linear analysis controls

The nonlinear transient analysis in LUSAS was performed by means of two load cases. The first load case consisting of one time step (0.001 of the total response time) was applied to establish a starting condition; the remainder of the transient analysis for the total response time was described by a second load case, proceeded from the starting condition. The total response time was determined from the experimental results shown in table 3.2. The dynamic analysis was performed using the implicit method, which requires the inversion of the stiffness matrix at every time step and therefore relatively expensive, but is unconditionally stable. An updated Lagrangian approach was selected to capture geometric and material nonlinearity and prevent mesh penetration (LUSAS, 2008). A solution for each time step was deemed acceptable; when the following convergence criteria were met: (a) the residual force norm (the limit for the sum of the squares of all residual forces as a percentage of the sum of the squares of all external forces, including reactions) ≤ 0.1, (b) the incremental displacement norm (the limit for the sum of the squares of the iterative displacements as a percentage of the sum of the squares of the total displacements) ≤ 1, and (c) the maximum number of iterations per time step was set to 12.

## 4.3 Results and observations

### 4.3.1 Stress distribution

The differences between the numerical solutions (elastic and visco-elasto-plastic) and the analytical solutions shown in Figure 4.4 and Appendix G, reveal that there is good agreement between the analytical models and the elastic numerical model with the exception of the stress concentrations at the edge of the adhesive. The analytical models seem to underestimate the stress concentrations. This general agreement is expected as the analytical models adopt an elastic constitutive model for the adhesive and should therefore be in perfect agreement with results obtained from the elastic numerical model.

The shear stresses in the adhesive obtained form the visco-elasto-plastic numerical solution also show good agreement with the elastic numerical and analytical solutions. As expected the peak stresses predicted by the visco-elasto-plastic numerical solution are closer to the elastic numerical solution at low loads (Figure 4.4), when the effects of plasticity are low. As the load increases the stress concentrations at the edges of the adhesive are reduced by the plastic deformation of the adhesive in these regions (Figures G1, G2, and G3). The stresses at the edges the adhesive drop considerably close to the failure (Figure G4). The viscous effects seem to have little influence on the stresses at these load durations.

Typical stress contours obtained from the nonlinear FE analysis are shown in Figure 4.5 and Figure 4.6. As expected the bulk of the adhesive in the SLS is subjected to a relatively uniform shear stress which increases rapidly toward the ends of the adhesive joint (Figure 4.5). The principal stresses observed in the T-peel stress contour plot (Figure 4.6) are also as expected with substantial lateral deformations due to Poisson's ratio effects. This corresponds to the deformations observed in the experimental investigations (Figure C6).

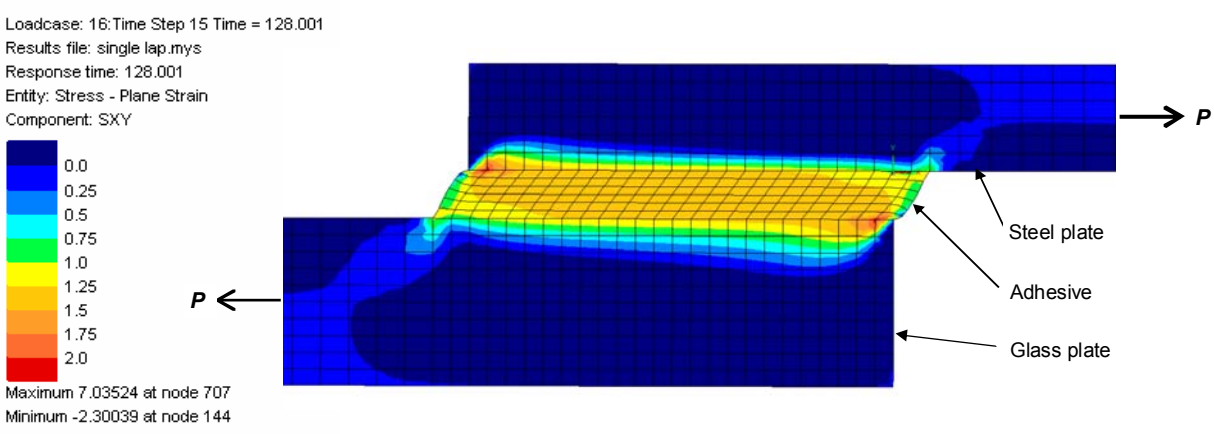


**Figure 4.5** Typical shear stress, $\tau_{xy}$, contours in the vicinity of the SLS adhesive joint with applied load *P* shown schematically. The results shown her are extracted from the SikaForce adhesive model with $\beta$=0.75 and *P* =1.818kN.

Glass failure, rather than adhesive joint failure was observed ion the SLS joints for the Holdtite and the Bohle adhesives. The stress distributions at high loads are therefore of interest for these adhesives and are shown in Figure 4.7 and 4.8. The maximum principal stresses on the glass surface shown in Figure 4.8 is 99.8MPa. This is the right order of stresses at which fully toughened glass is expected to fail and therefore confirms that the numerical analysis is sufficiently accurate at high loads.

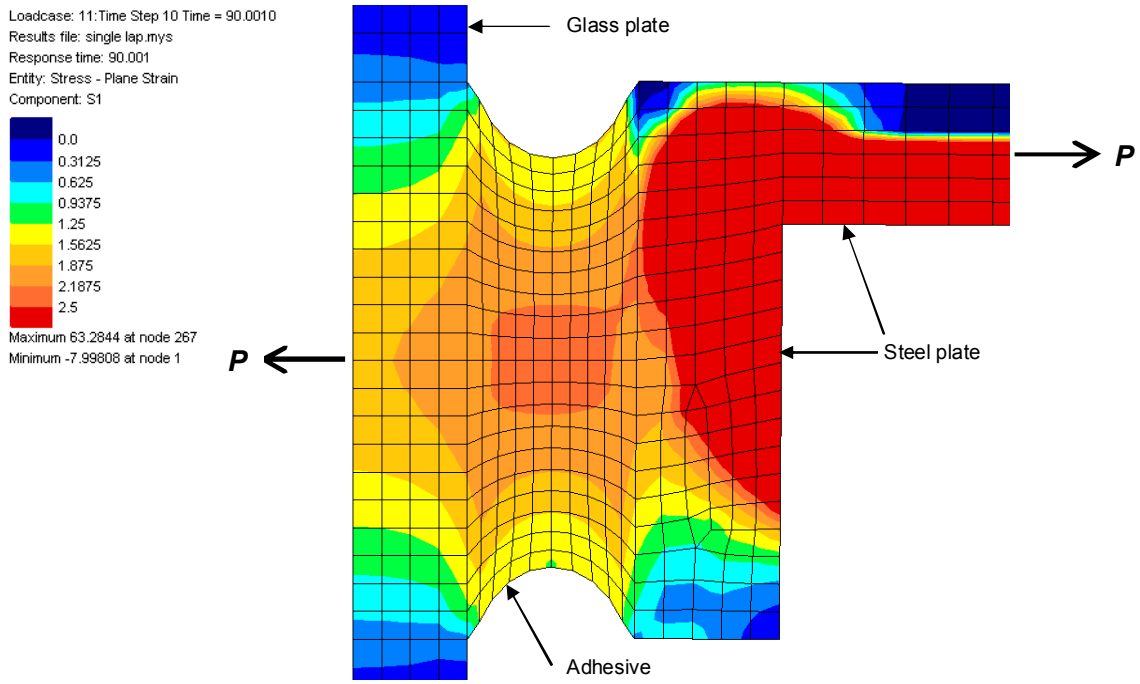


**Figure 4.5** Typical principal stress, $\sigma_1$, contours in the vicinity of the T-Peel adhesive joint with applied load *P* shown schematically. The results shown her are extracted from the DC993 adheisve with $\beta$=1.3 and *P* =1.78kN.

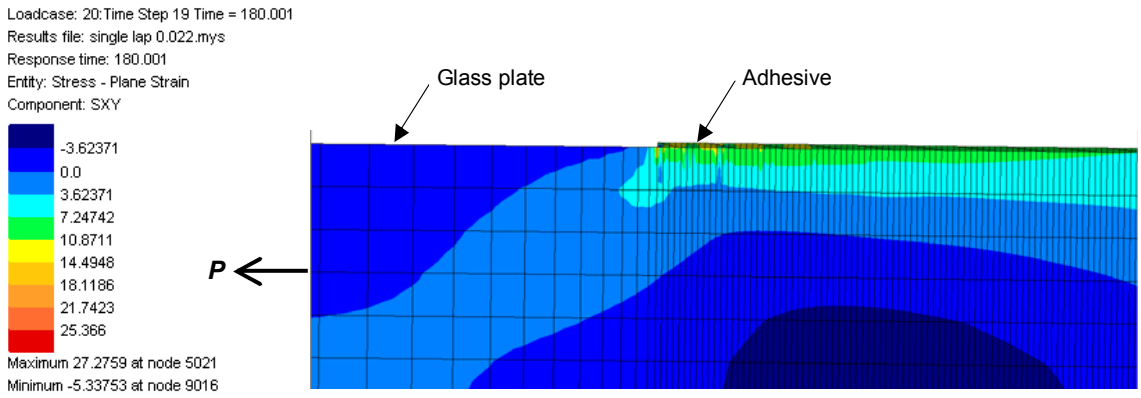


**Figure 4.7** Typical shear stress, $\tau_{xy}$, contours in the vicinity of the Bohle SLS joint with applied load *P* shown schematically and the steel plate omitted for clarity. The results shown here are for $\beta$=0.022 and *P* =11.493kN.

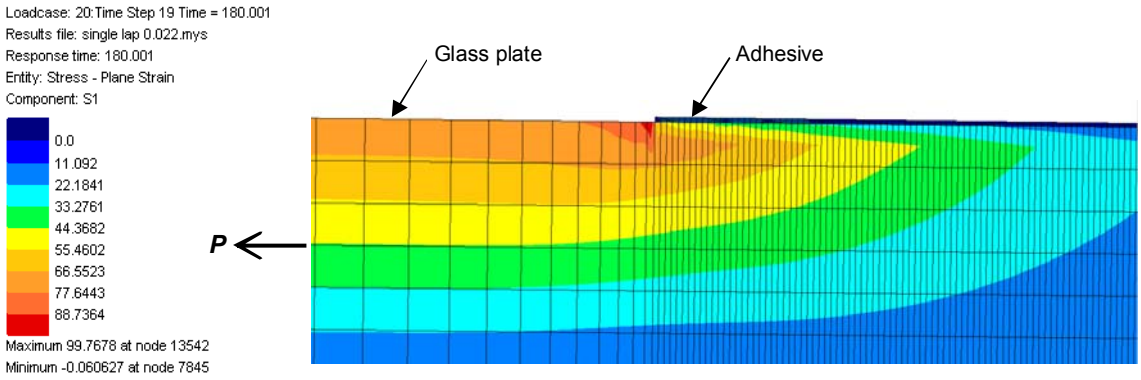


**Figure 4.8** Typical principal stress, $\sigma_1$, contours in the vicinity of the Bohle SLS joint with applied load *P* shown schematically and the steel plate omitted for clarity. The results shown here are for $\beta$=0.022 and *P* =11.493kN.

### 4.3.2 Load vs. displacement

The load *vs.* displacement results obtained from the nonlinear FE analysis are shown in Appendix F. The numerical results are superimposed on the experimental data to illustrate the goodness of fit between numerical predictions and experimental results.

The accuracy of the numerical model depends on two main factors: (a) the accuracy of the bulk adhesive properties obtained from the dumbbell specimens and (b) that the failure of the SLS and T-Peel specimens occurs in the adhesive (i.e. cohesion failure rather adhesion failure). The results shown in Appendix G confirm this as the best agreement was obtained in the 3M SLS, the DC993 SLS, the DC 993 T-Peel and for the stronger of the SikaForce SLS specimens that failed in cohesion. There is a moderate to poor agreement in the other adhesives. This is due to one or more of the following: (a) the difficulty in preparing a good quality dumbbell such as for the Holdtite; (b) the premature failure triggered by adhesion failure; (c) premature failure caused by glass failure.

## 4.4 Conclusions

The analytical modelling of adhesive joints is a non-trivial undertaking. The models available to date are based on a number of simplifying assumptions, not least, the elimination of all viscous decay and plasticity effects, resulting in an elastic representation of the adhesive. This means the analytical models described in this chapter, may be suitable for approximate design purposes, particularly for long duration loads on ductile adhesives, but are potentially unsafe for detecting failure triggered by the stresses peaks at the edges such as glass failure and failure of more brittle adhesives.

Constructing a close-to-reality numerical model of an adhesive joint is an equally demanding task and must be accompanied by a step-by-step validation of the model. The accuracy of the model also requires a careful determination of the material properties such as the decoupling of the transient visco-elastic properties from the time-invariant elasto-plastic properties. By carrying these tasks out correctly it is however possible to obtain a very good agreement between numerical and experimental results to the point of maximum load. This was observed for the 3M SLS, the DC993 SLS, the DC 993 T-Peel and for the stronger of the SikaForce SLS specimens.

Modelling of the post-failure performance of the adhesive was not attempted in this study. Although theoretically possible, it would be expected to add several complexities to the numerical analysis.

# 5 Conclusions and Recommendations

The principal aim of this study was to provide initial data on the structural performance of five candidate adhesives for steel-to-glass connections. The intention was that the performance data from this study would provide useful information for numerical or analytical calculations for such joints and would serve as a basis for identifying the adhesives on which further tests would be carried out. This aim has been achieved successfully. The quantitative structural performance data is provided in the preceding sections of this report and in the appendices. In addition, there are some general conclusions on the use of steel-glass adhesives listed here:

1. Some of the bulk material properties of adhesives such as Poisson's ratio and viscous decay constant are generally not available and require carefully controlled preliminary tests on dumbbell specimens. It is not always possible to produce good quality dumbbell specimens with some of the adhesives These mechanical properties are essential for constructing close-to-reality numerical models.
2. Adhesives are generally sensitive to surface preparation, but some adhesives, generally the thin joint / contact adhesives are very sensitive to adhesive thickness and surface roughness.
3. The adhesives investigated in this study have very different shear moduli with one adhesive being 12,500 stiffer than the most flexible adhesive. Despite the different chemical compositions, the elastic shear moduli, Gv, of the different adhesives seem to be related to the bond thickness, t, such that $G_v \propto e^{-t}$.
4. The stiffer adhesives tended to exhibit less ductility than the adhesives with low stiffness.
5. Analytical formulations are unsuitable for predicting the peak stresses at the edge of the adhesive joint and are therefore unsafe when brittle failure is expected.
6. Accurate numerical modelling through the finite element method is possible, but the complexity of capturing the transient nonlinear behaviour (caused by visco-elasticity, elasto-plasticity and large shear deformations) requires step-by-step validation of the model. Furthermore the numerical model is very sensitive to variations in the bulk adhesive properties which are sometimes difficult to obtain (see point 1 above).

The choice of adhesive for a steel-glass connection will depend on how well the adhesive meets the performance requirements of the proposed steel-glass connection. Since the precise performance requirements of the proposed steel-glass connection are as yet unknown we have provided a qualitative adhesive property table below that together with the quantitative data provided elsewhere in this report will be useful in selecting a suitable adhesive for this application.

**Table 5.1** Qualitative comparison of adhesives

| *Property* | *Adhesive* | | | | |
|---|---|---|---|---|---|
| | ***DC993*** | ***SikaForce*** | ***Holdtite*** | ***3M*** | ***Bohle*** |
| Strength | low | low | high | med. | high |
| Stiffness | low | low | high | high | high |
| Viscous decay | low | low | high | high | high |
| Ductility | high | high | low | med. | v. low |
| Ease of preparation | med. | low | high | high | low |
| Ease of tooling | med. | med. | high | high | med. |
| Variability (SLS) | low | high | low | low | high |
| Variability (T-Peel) | med. | med. | low | high | low |

From this table it may be concluded that the best adhesive for a low strength / low stiffness steel-glass joint is the DC993. In the event that a stiffer / stronger joint is required the two adhesive to consider are the Holdtite and the 3M. It is however important to note that this recommendation is based on the adhesives' performance under short duration loads in a laboratory environment. This recommendation and the use of the data in this report should therefore be limited to preliminary adhesive selection. Any use of these adhesive in real-world applications should be preceded by long term performance testing such as long duration loading, cyclic loading, exposure to aggrieve environments such as pollutants, cleaning agents, freezing / thawing cycles, UV etc.

## References


Adams R. *Adhesive Bonding*, Cambridge: Woodhead Publishing Limited, 2005.

ASTM. (1993). D 1876-93 Standard Test Method for Peel Resistance of Adhesives (T-Peel Test). *ASTM Standards* .

ASTM. (1999). D 1002-99 Standard test Method for Apparent Shear Strength of Single-Lap-Joint Adhesively Bonded Metal Specimens by Tension Loading (Metal-to-Metal). *ASTM Standards* .

Bigwood D. A. and Crocombe A. D. (1989) "Elastic analysis and engineering design formulae for bonded joints," *International Journal of Adhesion and Adhesives*, vol. 9, pp. 229-242.

BSI. (1996). Plastics - Determination of tensile properties - Part 1: General principles - BS EN ISO 527-1:1996. British Standard (pp. 1-16). BSI.

BSI. (1996a). Plastics - Determination of tensile properties - Part 2: Test conditions for moulding and extrusion plastics - BS EN ISO 527-2:1996 (pp. 1-14). BSI.

BSI. (2008) Bright Steel Products. Tecnical delivery conditions. Steels for quenching and tempering - BS EN 10277-5:2008 British Standard (pp. 1-16). BSI

BSI. (2004) Glass in Building. Thermally toughened soda lime silicate safety glass. Evaluation of conformity/product standard - BS EN 12150-2:2004 British Standard (pp. 1-42). BSI

Her S. (1999) "Stress analysis of adhesively-bonded lap joints," *Composite Structures*, vol. 47, pp. 673-678.

LUSAS (2008) LUSAS modeller on-line help.

Tsai M.Y., Oplinger D.W. and Morton J., (1998) "Improved Theoretical Solutions for Adhesive Lap Joints," *International Journal of Solids and Structures*, vol. 35, pp. 1163-1185.

## Appendix A – Test Geometries

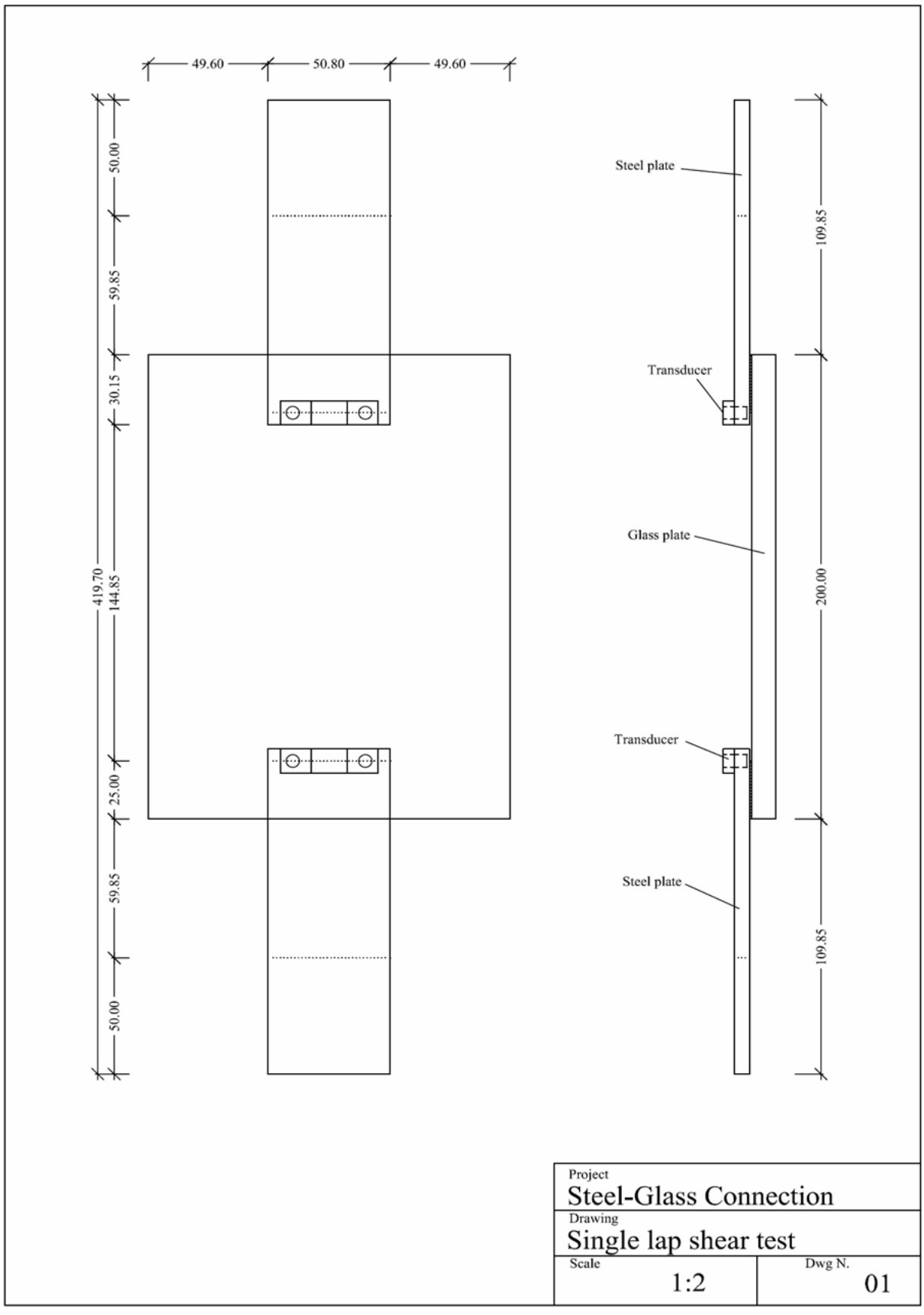

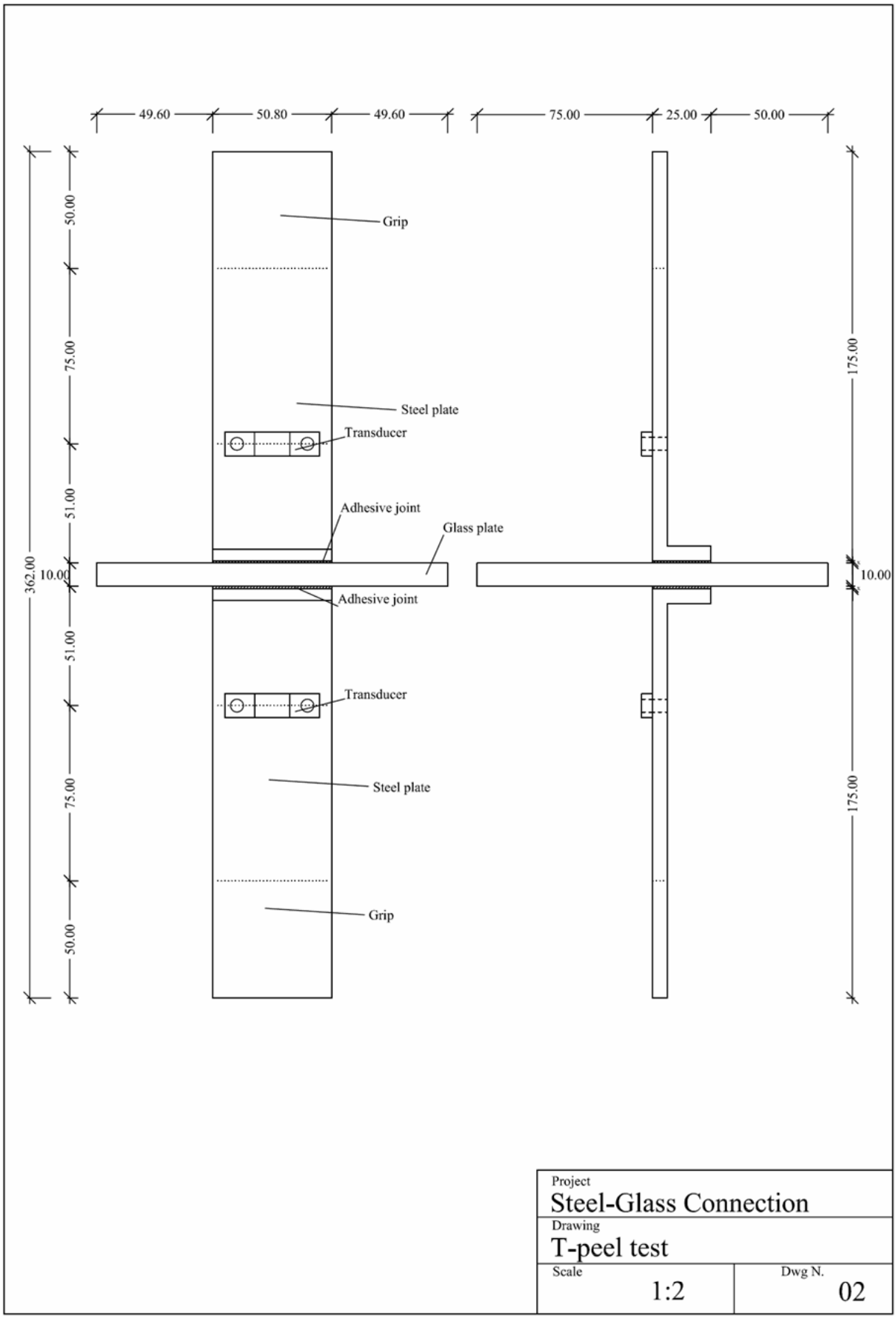
49.60
50.80
49.60
75.00
25.00
50.00
362.00
50.00
75.00
51.00
10.00
51.00
75.00
50.00
175.00
175.00
10.00
Grip
Steel plate
Transducer
Adhesive joint
Glass plate
Adhesive joint
Transducer
Steel plate
Grip
Project
Steel-Glass Connection
Drawing
T-peel test
Scale
1:2
Dwg N.
02

# Appendix B – Experimetal Results Graphs

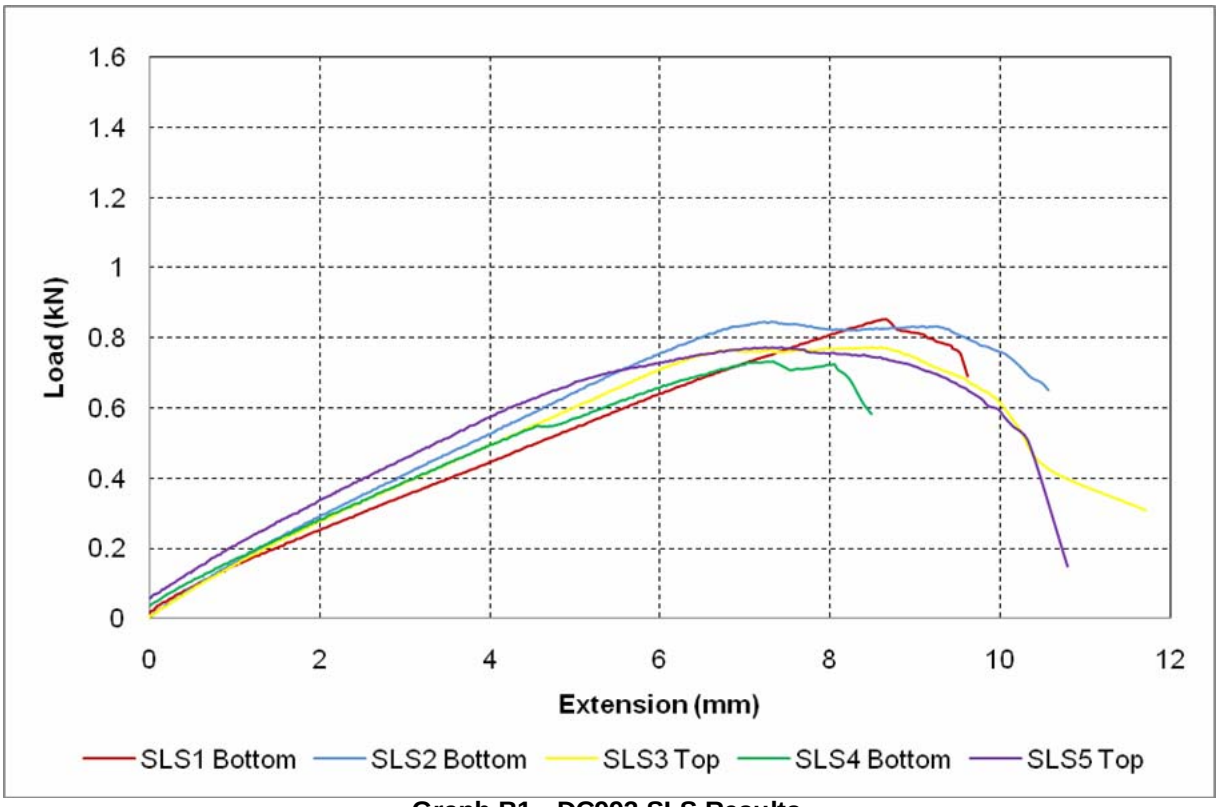


**Graph B1 - DC993 SLS Results**

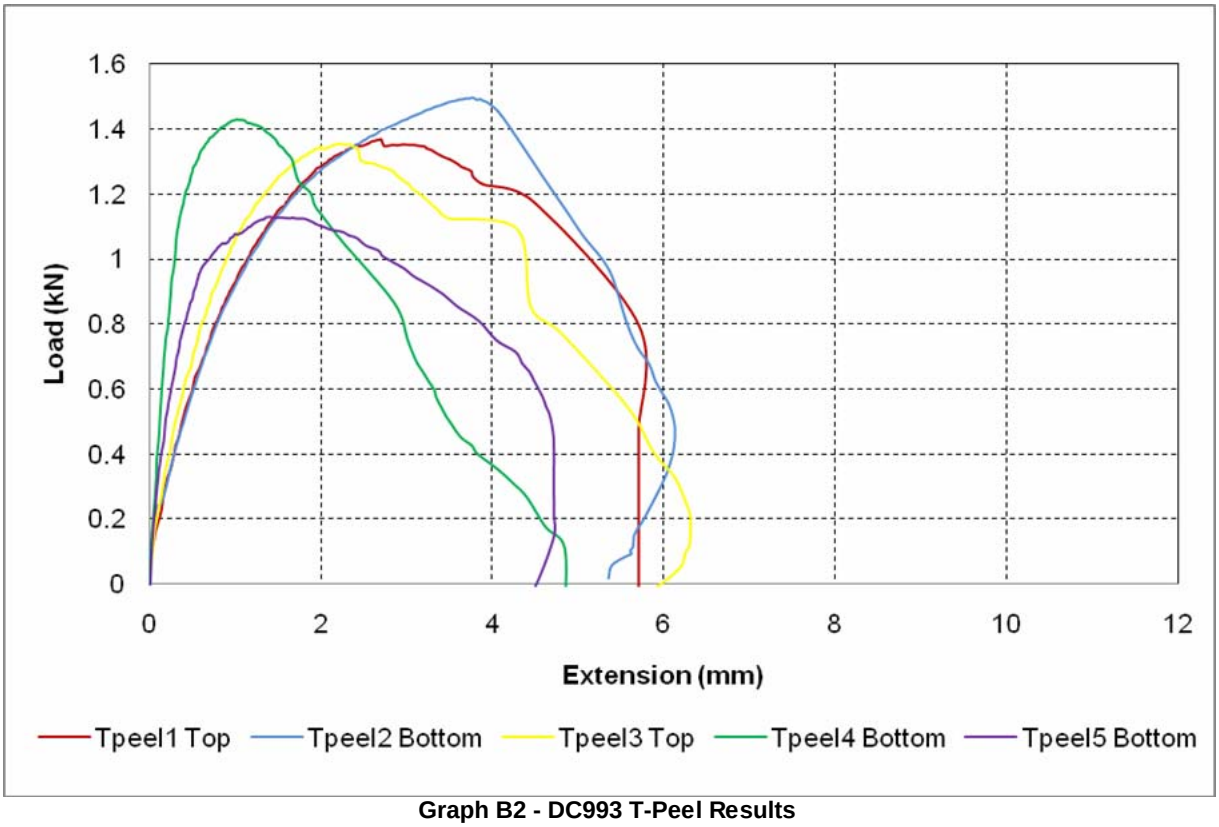


**Graph B2 - DC993 T-Peel Results**

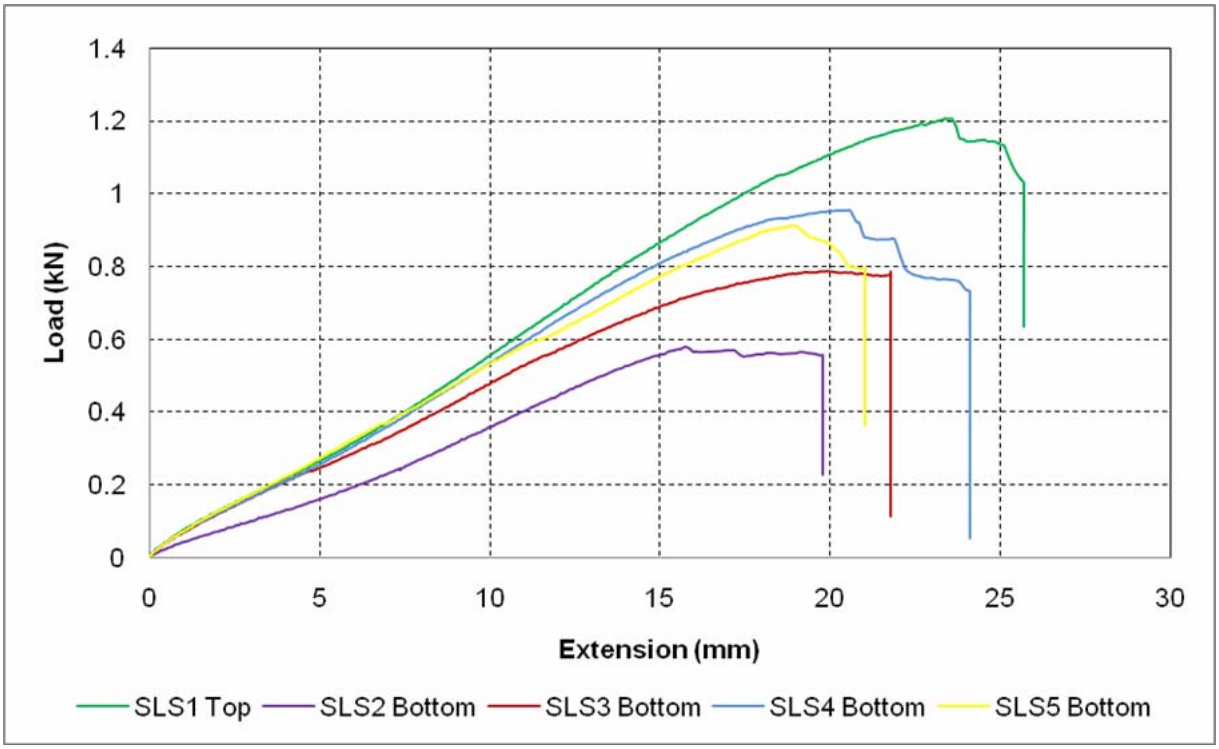


**Graph B3 - DC895 SLS Results**

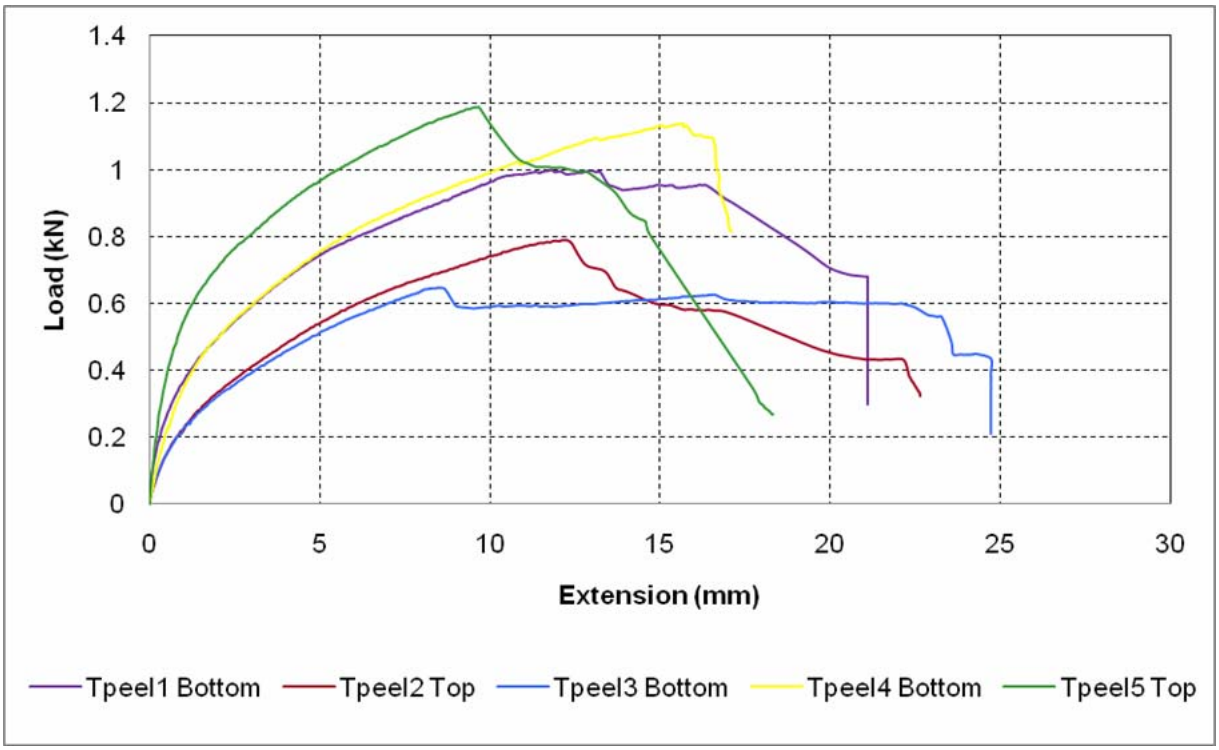


**Graph B4 - DC895 T-Peel Results**

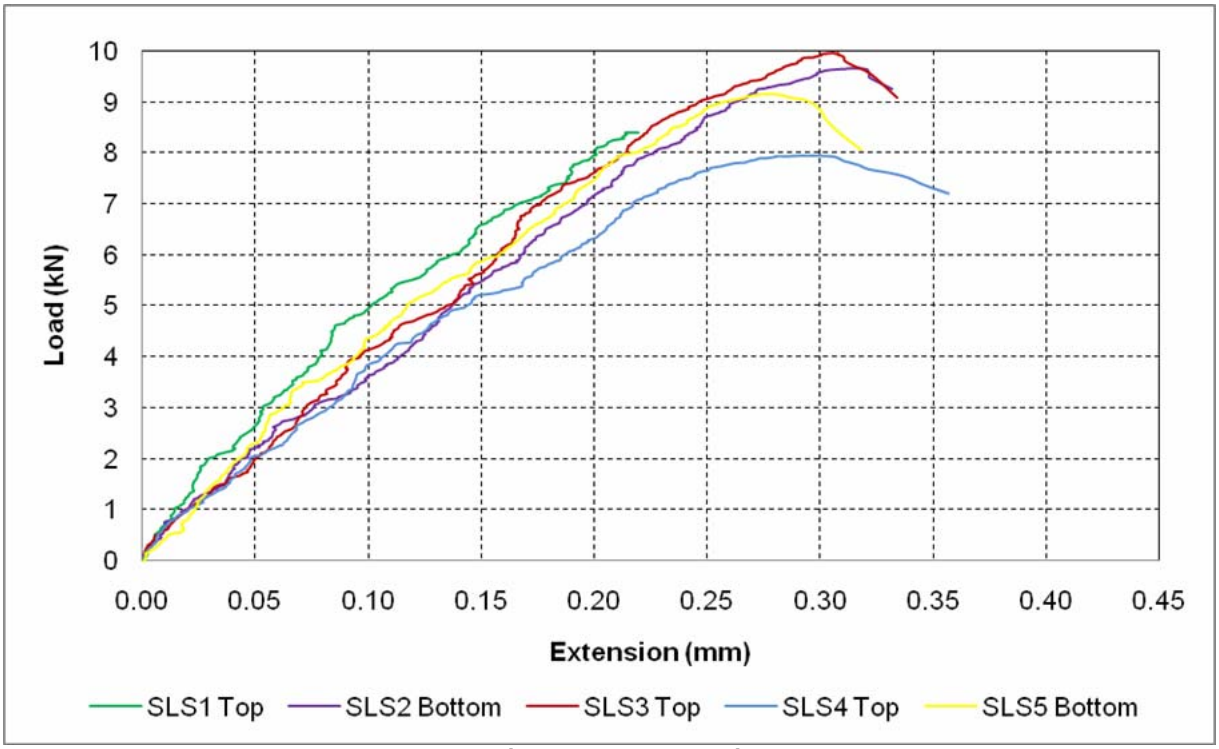


**Graph B5 - 3M SLS Results**

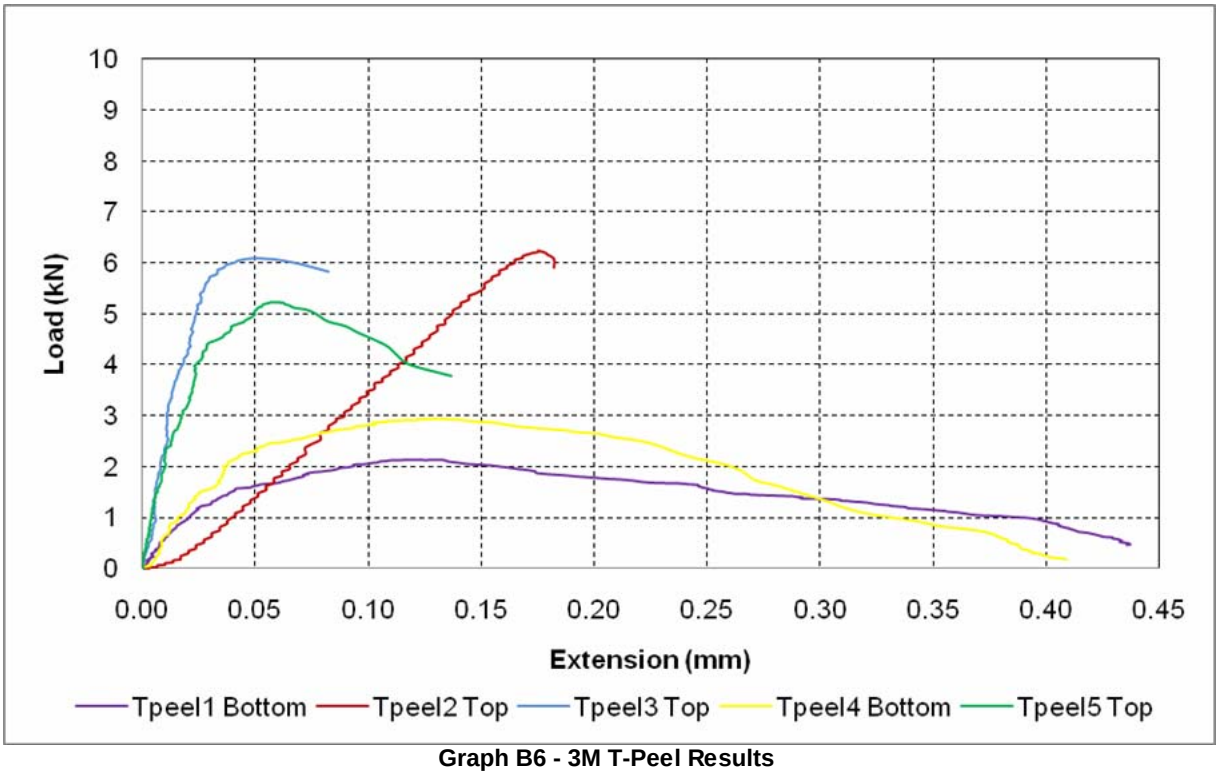


**Graph B6 - 3M T-Peel Results**

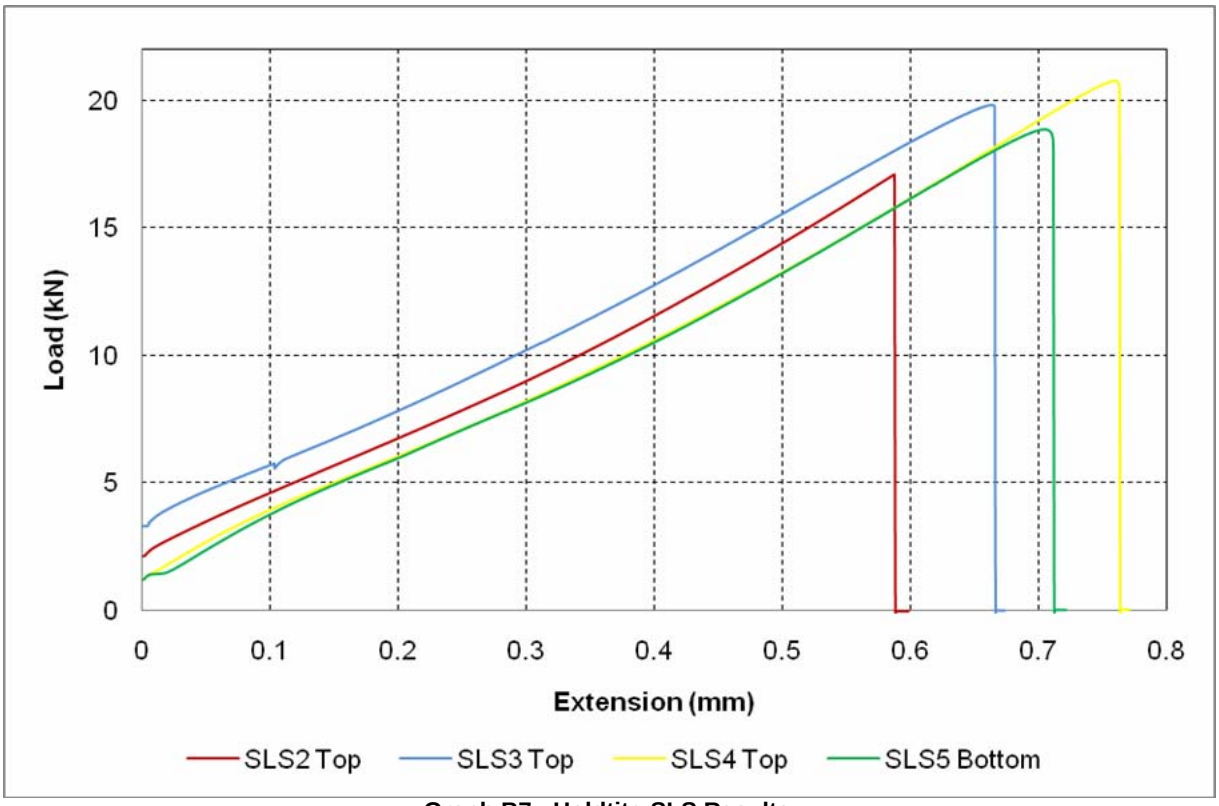


**Graph B7 - Holdtite SLS Results**

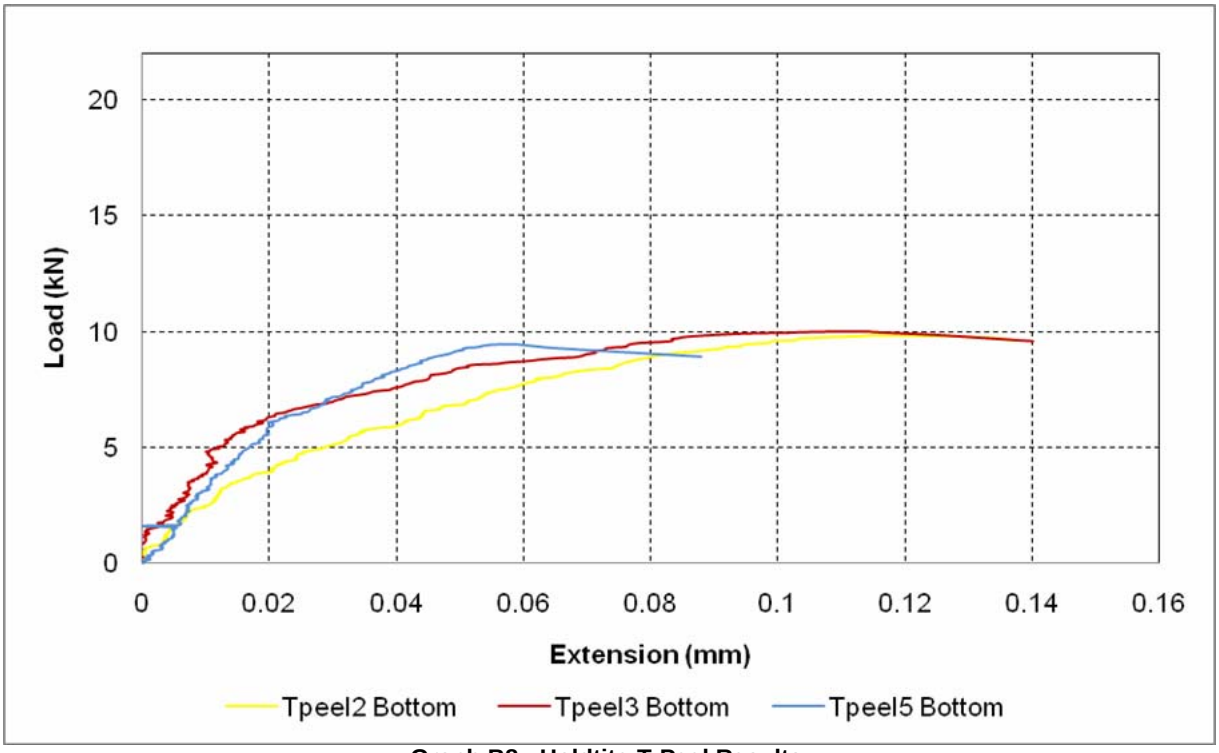


**Graph B8 - Holdtite T-Peel Results**

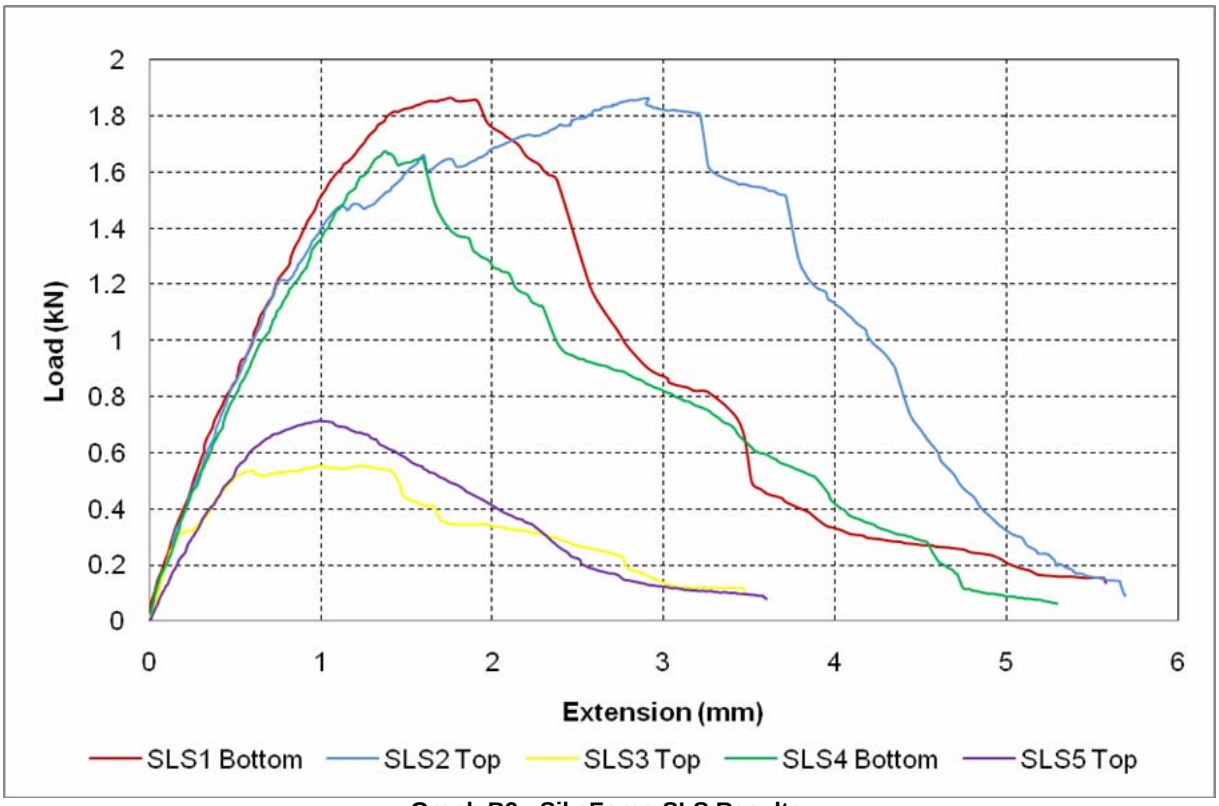


**Graph B9 - SikaForce SLS Results**

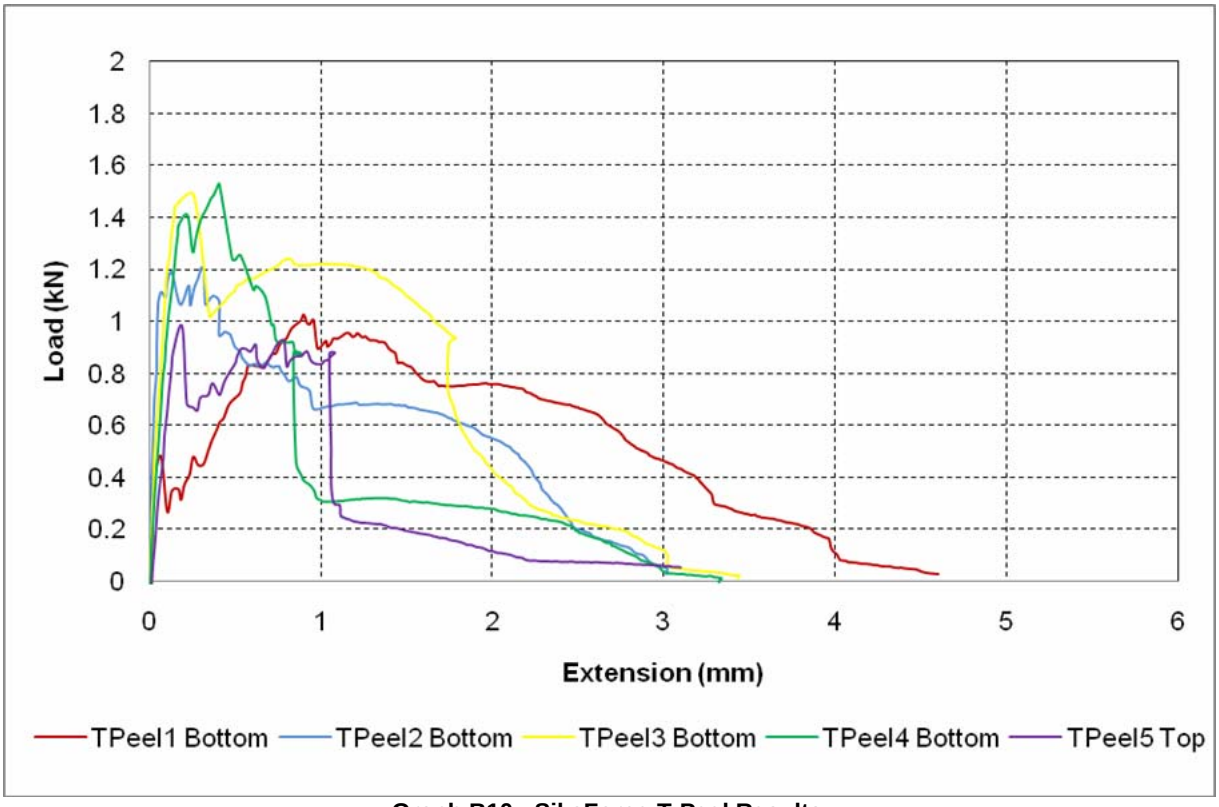


**Graph B10 - SikaForce T-Peel Results**

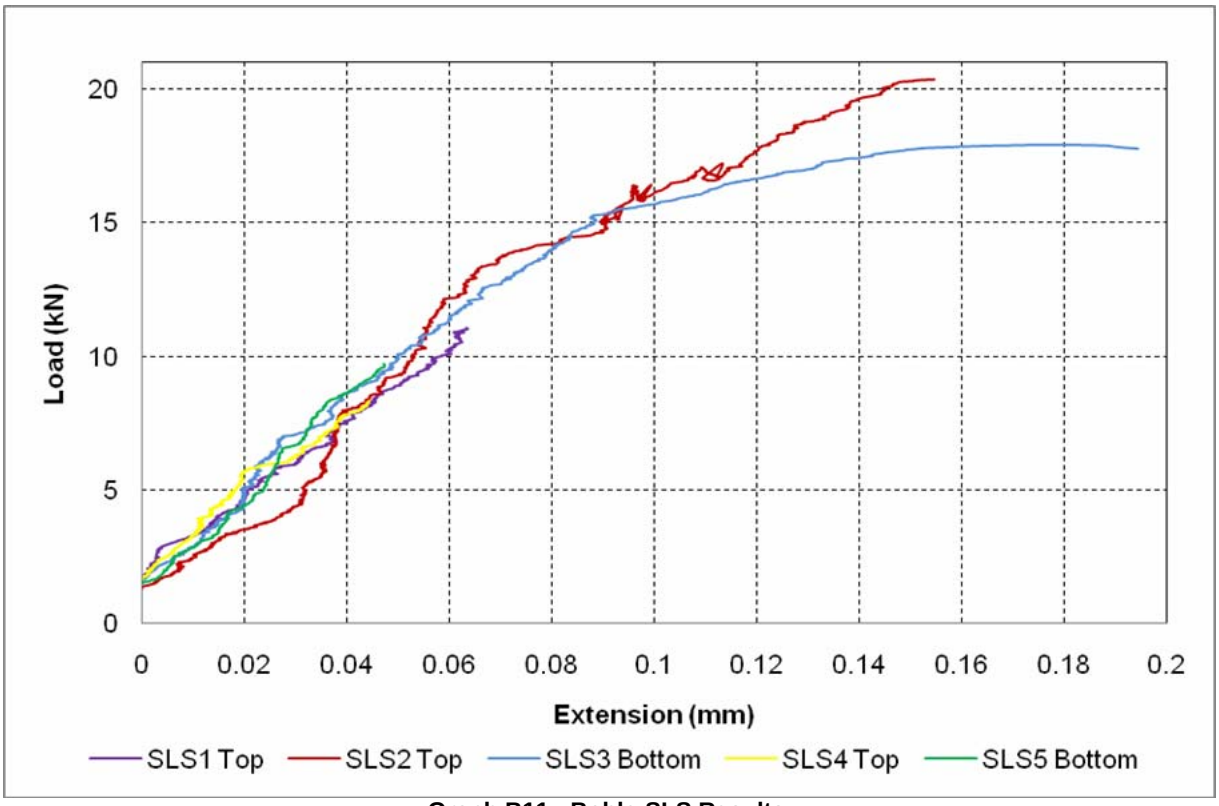


**Graph B11 - Bohle SLS Results**

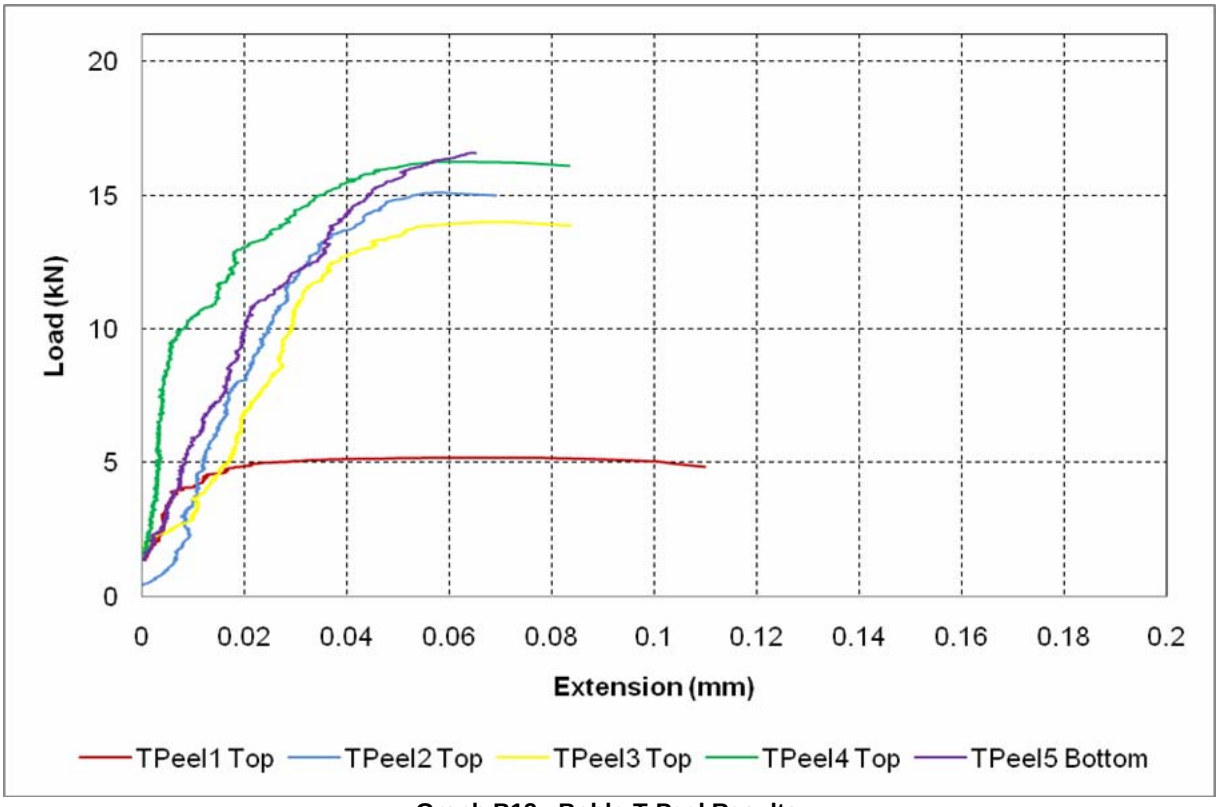


**Graph B12 - Bohle T-Peel Results**

## Appendix C – Images of Test Specimens

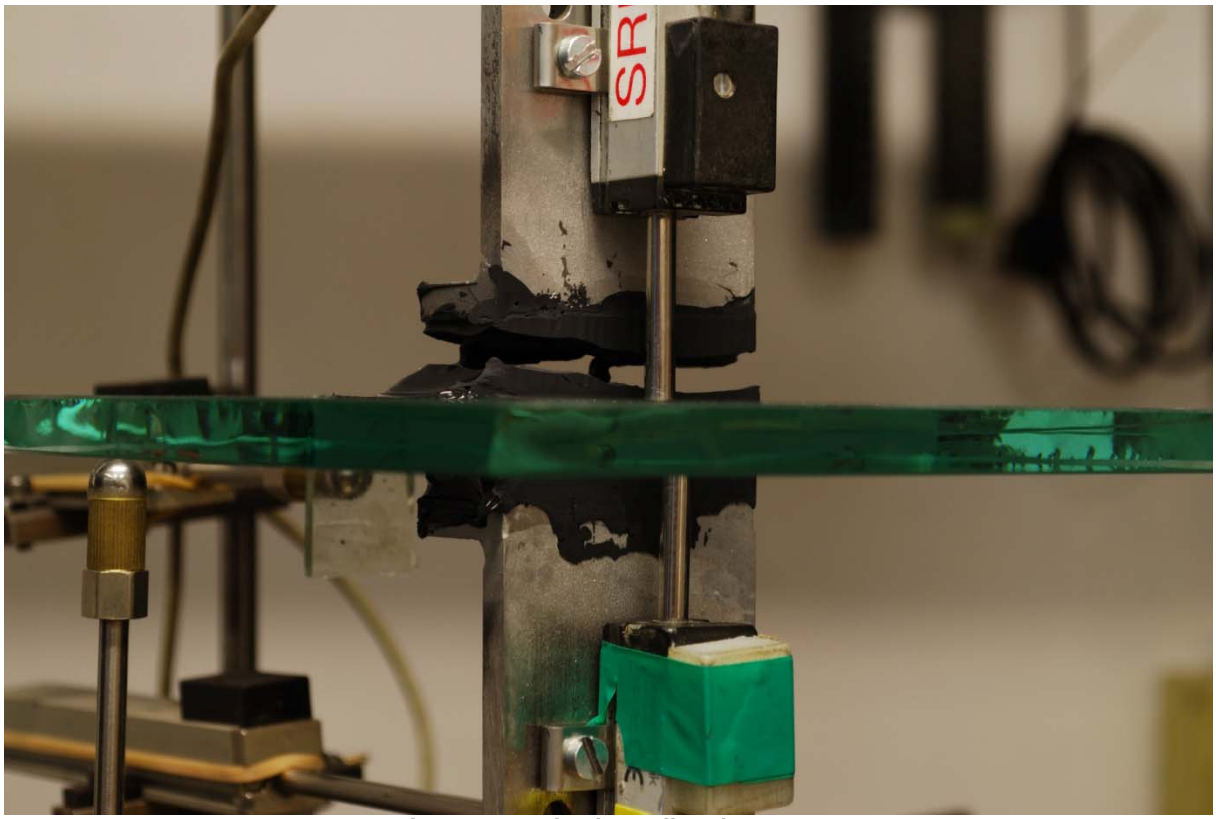

**Figure C1- Cohesive Failure in DC993**

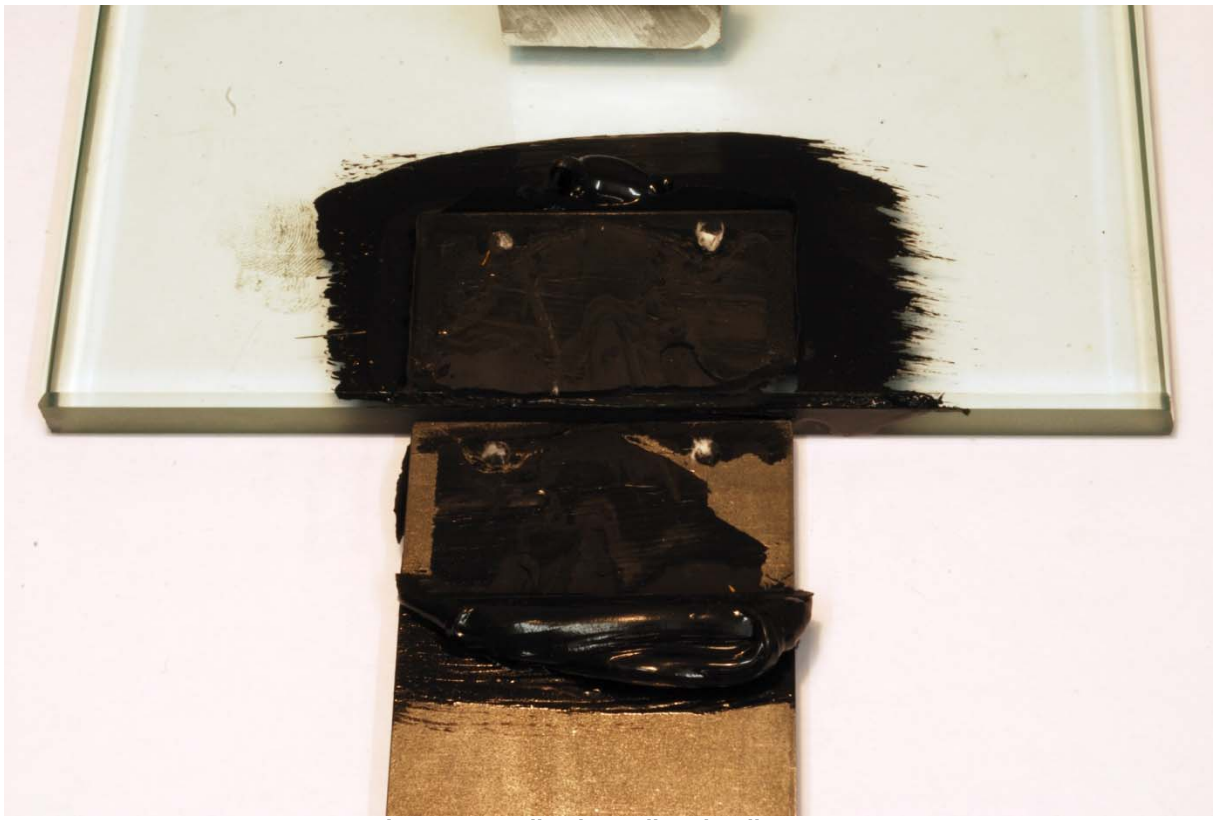

**Figure C2 - Adhesive Failure in SikaForce**

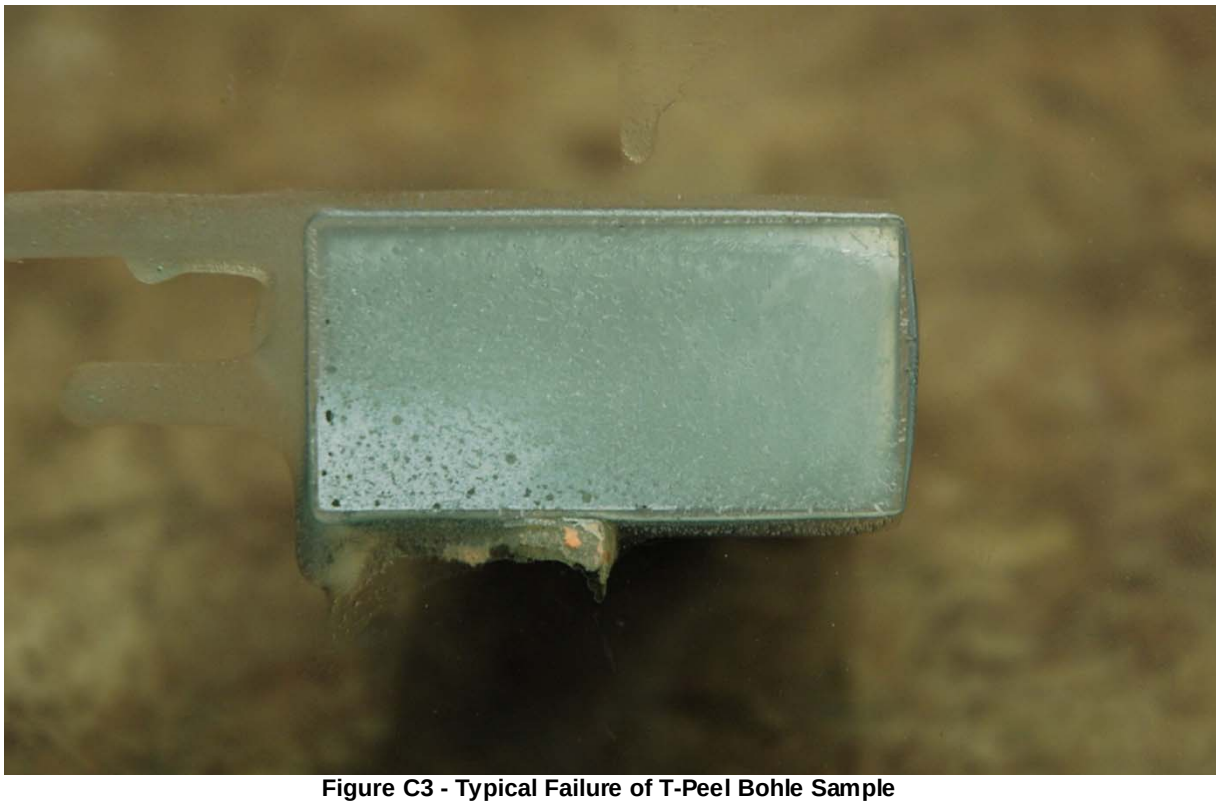

**Figure C3 - Typical Failure of T-Peel Bohle Sample**

**Figure C4 - Failure of Glass in a Holdtite Sample**

**Figure C5 - Failure of 3M T-Peel Sample**

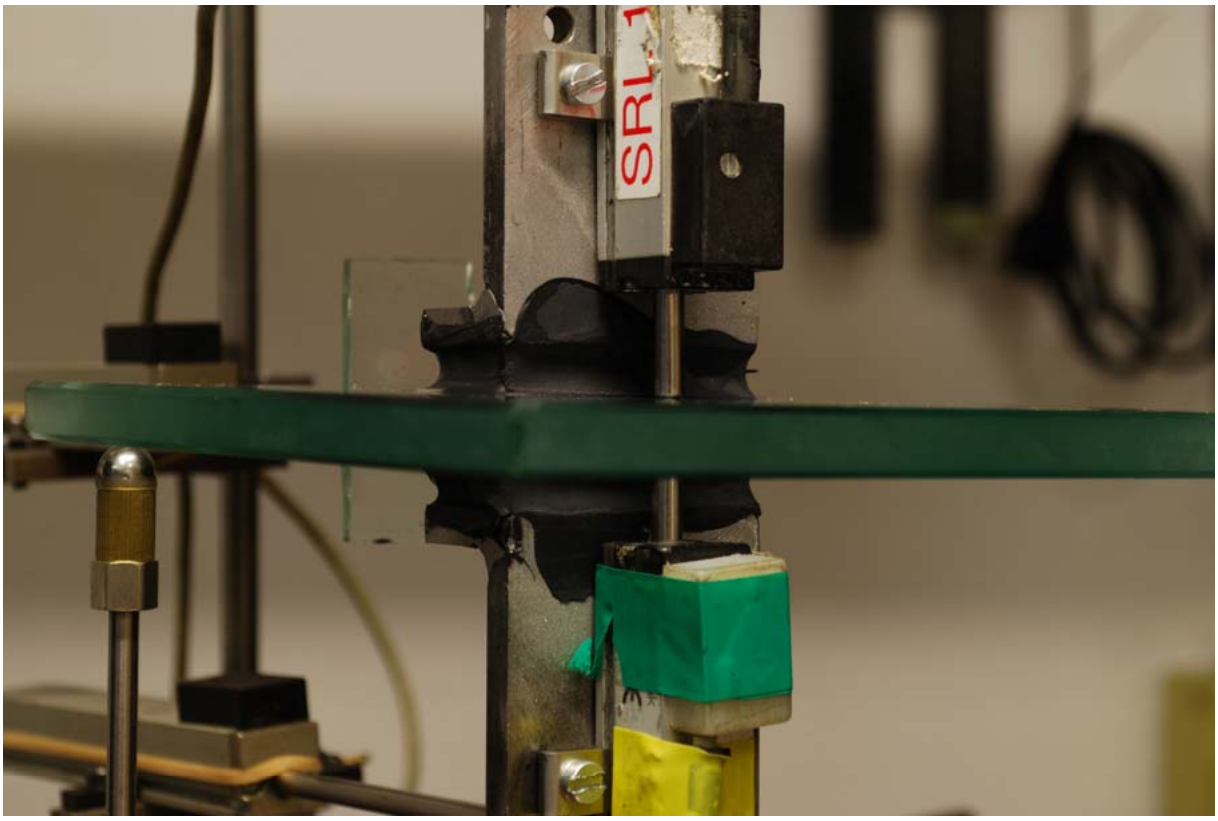


**Figure C6 – Loaded DC993 T-Peel Sample**

# Appendix D – Extended Sample Preparation

## D1 Surface Preparation, Cleaning & Priming

### D.1.1 Surface Roughness

The adhesive that required the most careful control was the UV curing acrylic, (Bohle B 682-T). For this adhesive the manufacturer specifies a bond thickness of 0.1 - 0.5mm, however information on the ideal surface roughness of the adherends was not readily available. In order to guarantee the optimum strength we therefore attempted to recreate the surface properties of a Bohle certified fitting on the steel adherends (by grinding). To measure the surface roughness a surface profiler (Form Talysurf 120) was used and standard measures ($R_a$ and $R_q$) were used to compare the different surfaces.

The average values for these surface roughness measurements are shown below in D1:

**Table D1** Surface Properties of Steel for Various Treatments

| | $R_a$ (μm) | $R_q$ (μm) | Max Deviation from Mean (μm) |
|---|---|---|---|
| Untreated Steel | 4.97 | 6.27 | 24.42 |
| Sanded Steel | 0.47 | 0.66 | 4.91 |
| Bohle Fitting | 0.30 | 0.37 | 1.38 |
| Ground Steel | 0.20 | 0.27 | 1.60 |

The ground steel fitting therefore provides a good match to the Bohle fittings. Example plots of typical surface profiles are shown below in Figures D1, D2 & D3 for some of the above finishes. The 3M and Holdtite adhesives also required a well controlled surface finish but this could simply be recreated by lightly sanding the surface with 180 grade sandpaper.

### D.1.2 Priming

Cleaning for the samples was as stated in 3.1.2 but the DC993 and SikaForce adhesives required additional treatment. These adhesives required primers – the SikaForce had two separate procedures whereas the DC993 only required one. For the SikaForce the surfaces were wiped with Sika Activator a solvent based cleaning agent designed to improve adhesion. This was left (for approximately 15 minutes) until dry and then a primer was applied and left to dry (Sika Primer-206 G+P – a pigmented solvent-based polyisocyanate

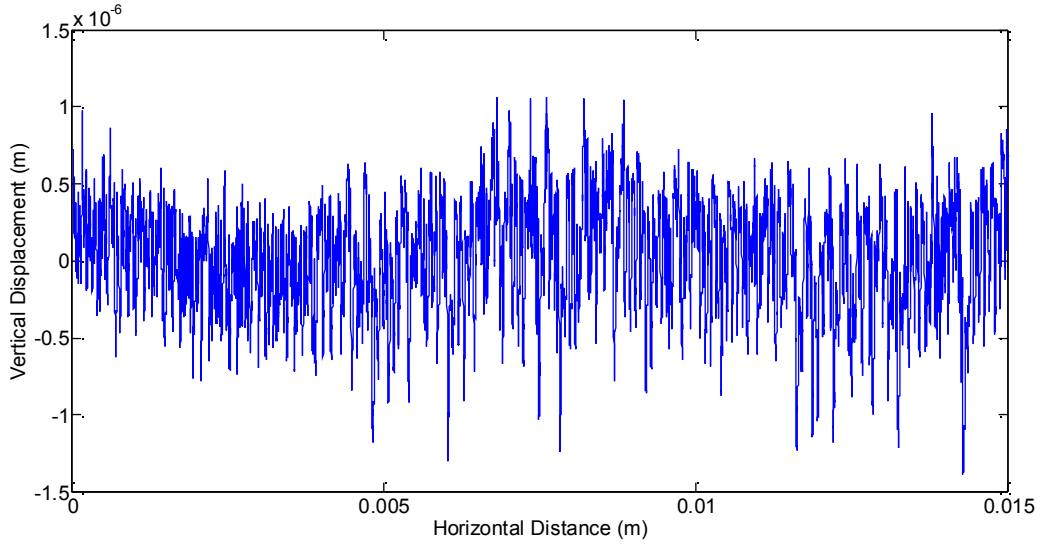


**Figure D1** Typical Surface Profile of Bohle Fitting

solution). For the DC993, a primer (Dow Corning 1200 OS Primer – A siloxane based solvent) was applied, by brush, to the steel alone and left to dry. The manufacturer's guidelines were followed explicitly for these products before the adhesives were used.

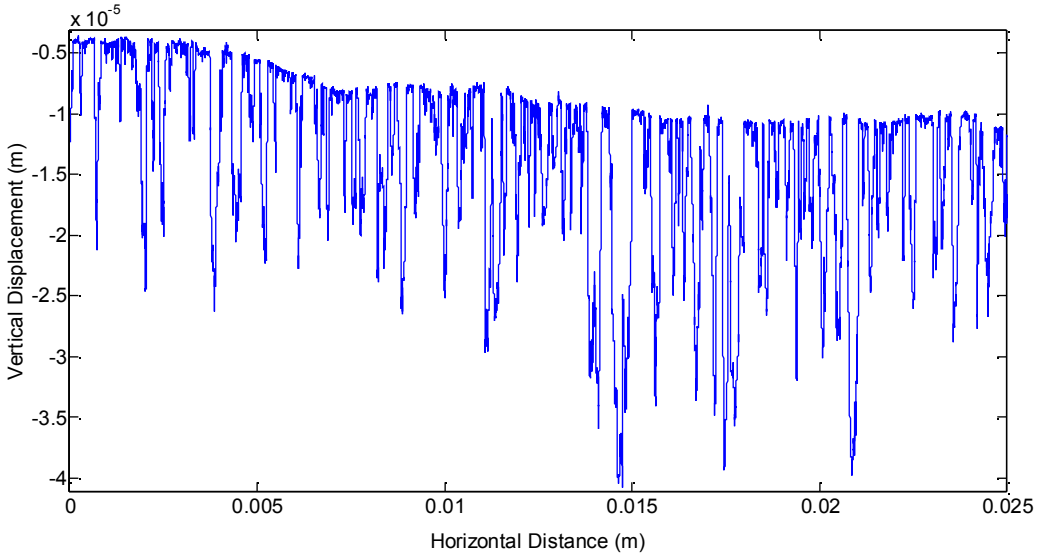


**Figure D2** Typical Surface Profile of Untreated Steel

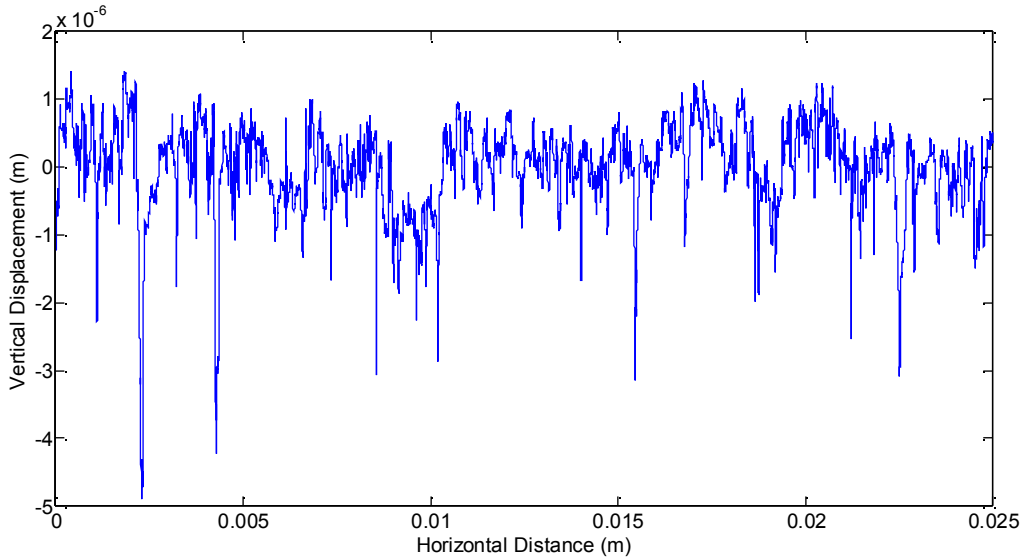


**Figure D3** Typical Surface Profile of Ground Steel

## D.2 Adhesive Mixing, Assembly Jigs & Assembly Process

### D.2.1 Mixing & Assembly Jigs

The DC895 and Bohle adhesives required no mixing at all and could simply be applied directly to the surfaces. However, all of the other adhesives required different mixing procedures.

The SikaForce was relatively straightforward but required proprietary pneumatic dispensing equipment (See Figure D4). The cartridges are placed in the dispenser and both components are forced through a static mixer attached to the end of the cartridges to ensure proper

mixing. The Holdtite and 3M were simply squeezed into a disposable measuring cylinder in the correct proportions and then mixed thoroughly by hand until neither of the individual components could be identified.

The DC993 required the most time and specialist equipment (see Figure D5) to mix it thoroughly. The silicone rubber was placed in a specially designed clamp and the catalyst was squeezed into the top of the cartridge. Then the two components were mixed together for 90 seconds using a fitting attached to an electric drill at a constant speed. Once complete, the cartridge was reassembled and then inserted into a manual dispenser ready for use.

**Figure D4** Pneumatic Dispensing Gun & Static Mixer

**Figure D5** DC993 Mixing Equipment

The assembly jigs used for most of the adhesives positioned the steel in the correct place on the glass (see Figure D6). These were made from epoxy filled modelling board cut to size by CNC machines. In order to ensure that the surfaces were parallel, the jigs and materials were placed on a single piece of flat glass, which minimised misalignment. In addition, tape was placed on the jigs around the joints to ensure that the jigs were easy to separate from the sample once the adhesive had cured.

The jigs were redesigned for the DC993 in order to allow the preparation of five sample with one mix. These redesigned jigs involved spacers working off a straight edge placed on a level table and allowed all 5 samples for both test geometries to be assembled simultaneously. The T-Peel jig is shown in Figure D7.

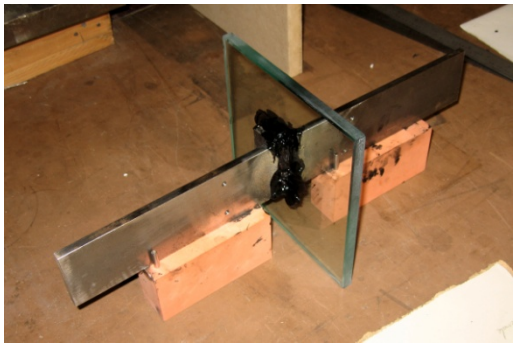

**Figure D6** T-Peel Assembly Jig

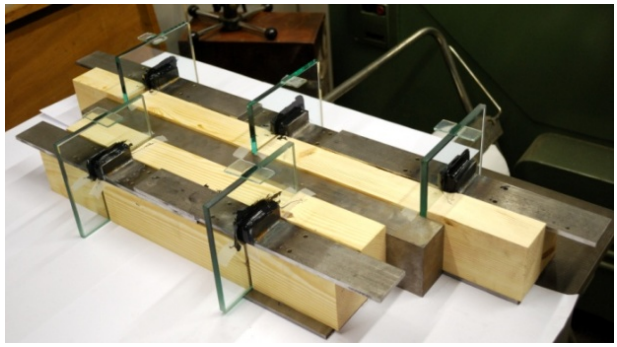

**Figure D7** DC993 T-Peel Assembly Jig

### D.2.2 Assembly Process

The thickness of the joints had to be carefully controlled to obtain the optimum strength, but this could only be achieved in the thick adhesives i.e. DC993 (6mm), DC895 (6mm), SikaForce (3mm) where flat glass spacers could be cut to size as the joint thickness was significant and the adhesives had gap filling properties.

However, for the Holdtite, 3M and the Bohle adhesives a more accurate technique was required as the joint thickness and tolerances were an order of magnitude smaller (0.1-0.2mm). For these adhesives, Spheriglass® glass microspheres (grade 2429 or 2024 - see datasheet in Appendix E – Product Datasheets) with known diameters were mixed in (<5% by volume) with the adhesive and then applied to the joint. Pressure was then applied to the surfaces, squeezing excess adhesive out the sides of the joint until contact was made with the glass spheres, guaranteeing the thickness of the bond width.

The thickness of each joint is specified in Table 3.1.

Once the surfaces were prepared, the adhesives were thoroughly mixed and the joint thickness could be controlled, the joints themselves were created. For the DC895, DC993 and SikaForce the adhesive was squeezed out of the cartridges, through the applicator and straight onto the substrates. It was important to ensure that there was significant adhesive present so that the correct joint thickness could be achieved. Pressure was then applied on the surfaces and onto the spacers with any excess adhesive being forced out the sides. As much of the excess was removed at the time as was possible without disturbing the components, and any remaining excess was carefully removed with a blade once cured. The same process was used for the Holdtite except the adhesive was spread onto the surface from the mixing container using a flat wooden applicator.

Manipulation of the metal and glass elements during the handling time was kept to a minimum to prevent imperfections such as air bubbles entering the joint.

There was a noticeable difference between the ease of application for each of the adhesives, in easiest-hardest – Bohle, Holdtite, 3M, DC895, DC993 then SikaForce. However, these observations do not necessarily carry through to assembly-line applications.

### D.2.3 Curing

For most of the adhesives the curing process required was to leave the samples in the jigs at a temperature of approximately 22°C and a relative humidity of 40% until the adhesive reached the handling time. The exception to this is the Bohle adhesive. This adhesive required UV radiation to cure. So the samples were placed under a high intensity UV bulb (Osram Ultra-Vitalux – 300W) at a distance of 10cm for a duration of 60 seconds to ensure that the adhesive had cured throughout.

The handling and curing times are shown in Table 3.1.

## Appendix E – Product Datasheets

**Product Information**

DOW CORNING

# DOW CORNING® 993
# Structural Glazing Sealant

### FEATURES

- Meets European standard for structural glazing as developed by EOTA working groups
- Excellent adhesion to a wide range of substrates including coated, enamelled and reflective glasses, anodised and polyester paint coated aluminium and stainless steel
- High level of mechanical properties
- Odorless and non-corrosive cure
- Excellent stability through wide temperature range: -50°C (-58°F) to 150°C (302°F)
- Resistant to ozone

### BENEFITS

- Structural capability
- The cured product exhibits excellent weathering characteristics, and a high resistance to ultra-violet radiation, heat and humidity
- Lot matching of base and curing agent not necessary
- Lot matching of base and curing agent not necessary

**Two-part silicone rubber**

### APPLICATIONS

- Two-part silicone sealant for structural glazing.

### TYPICAL PROPERTIES

Specification writers: These values are not intended for use in preparing specifications. Please contact your local Dow Corning sales representative prior to writing specifications on this product.

| Test method* | Property | Unit | Value |
|---|---|---|---|
| | **Base: as supplied** | | |
| | Color and consistency | | Viscous white paste |
| | Specific gravity | | 1.36 |
| | Viscosity ($100s^{-1}$) | mPa.s | 150,000 |
| | **Curing agent: as supplied** | | |
| | Color and consistency | | Viscous black paste |
| | Specific gravity | | 1.08 |
| | Viscosity ($100s^{-1}$) | mPa.s | 15,000 |
| ASTM D93 | Flash point - closed cup | °C | 28 |
| | | °F | 82.4 |
| ASTM D92<br>DIN 51376 | Flash point - open cup | °C | 84 |
| | | °F | 183.2 |
| | **As mixed** | | |
| | Color and consistency | | Black non-slump paste |
| | Specific gravity | | 1.33 |
| | Viscosity ($100s^{-1}$) | mPa.s | 40,000 |
| | Working time (25°C/77°F, 50% R.H.) | minutes | 10 to 30 |
| | Tack-free time (25°C/77°F, 50% R.H.) | minutes | 80 to 100 |
| | Corrosiveness | | Non-corrosive |
| | **As cured - after 7 days at 25°C (77°F) and 50% RH** | | |
| ISO 8339 | Tensile strength | MPa | 0.95 |
| ASTM D624 | Tear strength | kN/m | 6.0 |
| ISO 8339 | Elongation at break | % | 130 |
| ASTM D2240 | Durometer hardness, Shore A | | 40 |
| | Sealant dynamic design load | Pa | 140,000 |
| | Sealant static design load | Pa | 15,000 |
| | Service temperature range | °C | -50 to +150 |
| | | °F | -58 to +302 |

* ASTM: American Society for Testing and Materials.
ISO: International Standardization Organization.
DIN: Deutsche Industrie Norm.

## Product Information

DOW CORNING

# DOW CORNING® 895
# Structural Glazing Sealant

**One-part silicone rubber**

## FEATURES

- Meets the newly developed European standards for structural glazing application, as developed by EOTA
- Excellent adhesion to a wide range of substrates including coated, enamelled and reflective glasses, anodised and polyester coated aluminium profiles and stainless steel profiles
- Odorless and non-corrosive cure system
- One-component product
- Resistant to ozone and temperature extremes

## BENEFITS

- The cured product exhibits excellent weathering characteristics, and a high resistance to ultra-violet radiation, heat and humidity
- High ultimate tensile strength makes it ideally suited for structural bonding applications
- Excellent mechanical properties

## APPLICATIONS

- One component silicone sealant for structural glazing.

## TYPICAL PROPERTIES

Specification writers: These values are not intended for use in preparing specifications. Please contact your local Dow Corning sales representative prior to writing specifications on this product.

| Test method* | Property | Unit | Value |
|---|---|---|---|
| | **As supplied** | | |
| | Specific gravity | g/ml | 1.43 |
| | Slump or flow | mm | 0 |
| | Tack-free time (25°C/77°F, 50% R.H.) | minutes | 40 to 60 |
| | Cure schedule (25°C/77°F, 50% R.H.) | mm | |
| | - after 24 hours | | 2.2 |
| | - after 72 hours | | 3.5 |
| | (See also Optimal Glazing Conditions) | | |
| | **As cured - after 7 days at 25°C (77°F) and 50% RH** | | |
| ASTM D2240 | Durometer hardness, Shore A | Points | 38 |
| ASTM D0412 | Ultimate elongation | % | 600 |
| ASTM D0412 | Tensile strength, at 100% elongation | MPa | 0.7 |
| ASTM D0412 | Tensile strength, at ultimate elongation | MPa | 2.85 |
| ASTM D624 | Tear strength | kN/m | 19 |
| | **H-Piece Testing** | | |
| ISO 8339 | Ultimate elongation | % | 260 |
| ISO 8339 | Tensile strength | MPa | 1.06 |
| ISO 8339 | Young modulus | MPa | 1.0 |
| | Sealant dynamic design load | Pa | 140,000 |
| | Sealant static design load | Pa | 7,000 |
| | Service temperature range | °C | -50 to +150 |
| | | °F | -58 to 302 |
| | Working time | minutes | 15 |

* ASTM: American Society for Testing and Materials.
ISO: International Standardization Organization.

3M

# Scotch-Weld™

## Epoxy Adhesive

### 2216 B/A Gray • 2216 B/A Tan NS • 2216 B/A Translucent

**Technical Data** **March, 2002**

**Product Description**

3M™ Scotch-Weld™ Epoxy Adhesive 2216 B/A Gray, Tan NS and Translucent are flexible, two-part, room temperature curing epoxies with high peel and shear strengths.

**Advantages**

- Excellent for bonding many metals, woods, plastics, rubbers, and masonry products.
- Base and Accelerator are contrasting colors.
- Good retention of strength after environmental aging.
- Resistant to extreme shock, vibration, and flexing.
- Excellent for cryogenic bonding applications.
- 2216 B/A Gray Adhesive meets MIL-A-82720 and DOD-A-82720.
- 2216 B/A Tan NS Adhesive is non-sag for greater bondline control.
- 2216 B/A Translucent can be injected.

**Typical Uncured Physical Properties**

**Note: The following technical information and data should be considered representative or typical only and should not be used for specification purposes.**

| Product | 2216 B/A Gray | | 2216 B/A Tan NS | | 2216 B/A Translucent | |
|---|---|---|---|---|---|---|
| | Base | Accelerator | Base | Accelerator | Base | Accelerator |
| Color: | White | Gray | White | Tan | Translucent | Amber |
| Base: | Modified Epoxy | Modified Amine | Modified Epoxy | Modified Amine | Modified Epoxy | Modified Amine |
| Net Wt.: (lb/gal) | 11.1-11.6 | 10.5-11.0 | 11.1-11.6 | 10.5-11.0 | 9.4-9.8 | 8.0-8.5 |
| Viscosity: (cps) (Approx.) Brookfield RVF #7 sp. @ 20 rpm | 75,000 - 150,000 | 40,000 - 80,000 | 75,000 - 150,000 | 550,000 - 900,000 | 11,000 - 15,000 | 5,000 - 9,000 |
| Mix Ratio: (by weight) | 5 parts | 7 parts | 5 parts | 7 parts | 1 part | 1 part |
| Mix Ratio: (by volume) | 2 parts | 3 parts | 2 parts | 3 parts | 1 part | 1 part |
| Work Life: 100 g Mass @ 75°F (24°C) | 90 minutes | 90 minutes | 120 minutes | 120 minutes | 120 minutes | 120 minutes |

# UV adhesive B 682-T

Technical Data

## 1. Product Description

This UV curing adhesive is translucent but not completely clear. It is relatively thick-bodied (medium viscosity) and must therefore be applied to the bonding surface prior to assembling the parts. Due to the very high final strength of this adhesive, it is especially suitable for statically demanding bonds. Glass/metal bonds work out especially well - it is preferably used when bonding metal hinges to glass doors. Many other materials can be bonded with this adhesive: apart fom metal to glass, it is also suitable to bond stone, wood and variety of thermoplastics to glass.
As not all thermoplastics can be bonded, prior trilas are always recommended when working with these materials. The adhesive B 682-T also reacts without UV exposure when using the BOHLE UV activator LF (Art.-Nr. BO 52 093 65/BO 52 093 66) (e.g. for coloured glass, laminated glass, metal/metal bonds etc.). In this case please consider a slightly reduced final strength.

## 2. Fields of application

- especially for glass/metal bonds
- for bonds with demanding strength requirements

## 3. Suitable bonding materials

- glass metal
- glass to wood
- temp. glass to temp. glass
- glass to glass
- glass to stone
- glass to thermoplastics

## 4. Characteristics

| | |
|---|---|
| Material Basis | Acrylic-acid-ester |
| Colour | translucent |
| Refractive index | approx. 1.50 |
| Densitiy | approx. 1.10 g/cm³ |
| Solid content | 100% |
| Flash point | approx. 93°C |
| Viscosity | approx. 980 mPa·s |
| Consistency | medium viscous |
| Bond line | 0.1 - 0.5 mm |
| Irradiation | UVA 320 - 400 nm |
| Hardness | approx. 80 Shore D |
| Shear strength | approx. 26 N/mm² |
| Temperature range | -40°C to +140°C |
| Linear shrinkage | approx. 5% |
| Storage | In original container, dry and dark (no UV exposure) |
| Shelf life | 9 month |

## 5. Available packaging

| | | |
|---|---|---|
| UV-Adhesive B 682-T | 1000g bottle | Art.-No. 52 093 96 |
| UV-Adhesive B 682-T | 250g bottle | Art.-No. 52 093 95 |
| UV-Adhesive B 682-T | 100g bottle | Art.-No. 52 093 94 |
| UV-Adhesive B-682-T | 20g bottle | Art.-No. 52 093 93 |

## 6. Limitation of liability

Precautions see EU Safety Data Sheet.
The preceding information as well as any technical recommendation given in writing, verbally or based on tests are provided to the best of our knowledge. However, they are non-binding recommendations only and do not affect your responsibility to determine the correctness of given recommendations and suitability of the product for your particular purposes. The application, use or processing of our products as well as the production of products based on our technical recommendations are beyond our control and therefore fall exclusively in your area of responsibility. Sales of our products are effected according to our most updated General Sales and Delivery Conditions.

Bohle AG · DieselstraBe 10 · D-42781 Haan · T +49 2129 5568-0 · F +49 2129 5568-281

Macroplexx®
structural adhesives

# TDS 3295

## General Description

**MACROPLEXX® 3295** is a second generation acrylic adhesive, designed to combine high shear strength, with high temperature resistance, with the additional qualities of a rubber toughened adhesive. The adhesive works when mixed at a 1:1 ration trough a mix nozzle, as well as with a bead on bead application system. This adhesive has incredible adhesion on a wide variety of substrates, whilst maintaining very high peel and impact strengths throughout.

## Typical Applications

Sign Fabrication and Installation  Automotive Assembly  GRP Fastening Systems  Magnet Bonding

## Chemical Resistance

Excellent Resistant to:

- Hydrocarbons
- Acids and Bases (3-10 ph)
- Salt Solutions

## Packaging

- 25ml Syringe
- 50ml Cartridge
- 250ml Universal
- 400ml Cartridge
- Bulk Dispensing Systems

## Technical Features

| | |
|---|---|
| Part A Colour | Green |
| Part B Colour | Pink |
| Mixed Colour | Purple |
| Working Time | 2 Minutes |
| Fixture Time | 6 Minutes |
| Viscosity | 3500cps |
| Flash Point | 12°C |
| Specific Gravity | 1.02 |

## Application Instruction

Please consult Macroplexx application manual.

## Technical Notes

Macroplexx 3295 can be also applied at an offset ratio to increase the working time. The upper limit is 3.2 Part A to 1 Part B, which will allow 7 minutes open time, without any change in ultimate cured strength.

Macroplexx 3295 is suitable for paint bake cycles up to 180°C for 20 minutes.

## Typical Properties Cured Material

| | |
|---|---|
| 50% Ultimate Strength | 1 Hour |
| Full Cure | 6 Hours |
| Temperature Range | -35°C to 180°C |
| Gap Fill | 3mm |

## ASTM D1002 Lapshears (Tensile Result)

| | |
|---|---|
| Steel/steel | 20-35 N/mm$^2$ |
| Glass/Metal | 16-22 N/mm$^2$ |
| Polycarbonate* | 13 N/mm$^2$ |
| On ABS/ABS * | 8 N/mm$^2$ |

* Substrate failure

## Suitable Substrates

| | | | |
|---|---|---|---|
| Ferrites | Ceramics | Steel | Gelcoats |
| Acrylics | Urethanes | Aluminium | Polyesters |
| GRP | Vinyl | St.Steel | Wood |
| FRP | | | |

## Terminology

(1) Working/Open Time: The time interval between application of adhesive to substrate, and the possible assembly/repositioning of the two mating parts @ 20°C

2) Fixture Time: The length of time after the substrate assembly that will allow a joint to support a 1kg dead weight. (Tested on a 12mm x 25mm overlapped joint @ 20°C)

TDS 3295-5/6/2007

Holdtite
Portobello Industrial Estate, Birtley, County Durham, United Kingdom, DH3 2RE Tel: +44 (0)191 411 3191 Fax: +44 (0)191 411 3192
E-mail: info@holdtite.com Web: www.holdtite.com

Product Data Sheet
Version 2/9/08

# SikaForce®-7550 L15

## Elastic, Fast-curing and non-sagging assembly adhesive

Technical Product Data (typical values)

| Properties | Component A (Resin) | Component B (Hardener) |
|---|---|---|
| Chemical base | Polyols, filled | Isocyanate derivates unfilled |
| Color | Black | Whitish |
| Mixing Color | Black | |
| Cure mechanism | Polyaddition | |
| Density @ 25°C (77°F) (CQP[1] 553-1) | 1.33 g/cm³, approx. | 1.13 g/cm³, approx. |
| Solid Content | 100% | 100% |
| Viscosity (25°C) (CQP 539-1 / DIN 53019) | 25,000 mPas, approx. | 25,000 mPas, approx. |
| Mixing viscosity (CQP 539-1 / DIN 53019) | 170,000 mPas, approx. | |
| Mixing Ratio parts per weight | 100 | 42 |
| Parts per volume | 100 | 50 |
| Application temperature range | 15-30°C (59-86°F) | |
| Non-sag properties | Very good | |
| Open time[2] (maximum time between application of adhesive and assembly operation) (CQP 526-1) | 15 min. approx. | |
| Tensile lap-shear strength (CQP 046-1 / ISO 4587) | 5 MPa, approx. | |
| Strength development and curing speed according to tensile lap-shear strength[2] (CQP 046-1 / ISO 4587) | 2h<br>4h<br>24h | 0.20 MPa approx.<br>0.45 MPa approx.<br>1.90 MPa approx. |
| Shore-A hardness (CQP 023-1 / ISO 868) | 70, approx. | |
| Tensile strength (CQP 036-1 / ISO 37) | 5MPa, approx. | |
| Elongation at break (CQP 036-1 / ISO 37) | 350%, approx. | |
| Glass transition temperature (CQP 036-1 / ISO 4663) | -50°C (-58°F), approx. | |
| Volume resistivity (ASTM D 257-99) | $10^{13}$ Ωcm, approx. | |
| Service temperature (continuous) (CQP 513-1) | -40 °C to + 100 °C (-40°F +212°F), approx. | |
| Shelf life (stored in original closed packaging below 25°C) (CQP 016-1) | 6 months | |

[1] CQP= Sika Corporate Quality Procedure [2] 23°C (73°F) / 50% r.h.

Industry

### Description

SikaForce®-7550 L15 is a thixotropic 2-component assembly adhesive, which cures by chemical reaction of the two components to form a durable elastomer. It consists of a filled polyol based resin and an isocyanate based hardener. SikaForce®-7550 L15 is manufactured in accordance with the ISO 9001/14001 quality assurance system and the Responsible Care Program.

This product is suitable for experienced professionals only. Tests with actual substrates and conditions have to be performed to ensure adhesion and material compatibility.

### Product Benefits

- Cold applied and highly thixotropic
- Short cut-off string
- Fast cure and strength development independent to air humidity
- Elastic / good gap-filling capabilities
- Adequate working time to complete assembly, despite rapid cure
- Bonds well to a wide variety of substrates
- Withstands high dynamic stresses
- Vibration damping
- Electrically non-conductive
- Aging resistant
- Room temperature curing
- Solvent free

**Product Information**

DOW CORNING

# *Dow Corning*® 1200 OS Primer

## FEATURES

- Improves adhesion of silicone elastomers and foams to many substrates
- Provides more uniform and stronger bonds
- Easy to use
- Remains active over several hours after application
- Formulated for low toxicity, i.e. not a health hazard according to European directive 88/379/EEC
- Solvent used does not deplete the ozone layer
- Resistant to ozone, ultra-violet radiation and temperature extremes

## APPLICATIONS

Primer for silicone elastomers, silicone foams and adhesives/sealants

## TYPICAL PROPERTIES

Specification Writers: These values are not intended for use in preparing specifications. Please contact your local Dow Corning sales office or your Global Dow Corning Connection before writing specifications on this product.

| CTM* | ASTM* | Property | Unit | Value |
|---|---|---|---|---|
| | | **As supplied** | | |
| 0176 | | Color | | Colorless liquid |
| 0050 | D1084B | Viscosity at 23°C (73.4°F) | mPa.s | 1 |
| 0090A | D56 | Flash point - closed cup | °C | 27 |
| | | | °F | 80.6 |
| | D1298 | Specific gravity at 23°C (73.4°F) | | 0.82 |
| | | Non-volatile content | % | 5 |
| | | Solvent type | | Volatile siloxanes |

* CTM: Corporate Test Method, copies of CTMs are available on request.
ASTM: American Society for Testing and Materials.

## DESCRIPTION

*Dow Corning*® 1200 OS Primer is used to improve adhesion and accelerate adhesion build-up of silicone elastomers to various substrates. This moisture curing primer is supplied as a dilute solution of reactive materials in low viscosity siloxane.

## HOW TO USE

With most surfaces, substantially stronger and more uniform bonds are obtained by preparing them with a primer prior to the application of the silicone elastomer. For obtaining best results, the following steps should be followed on all surfaces except silicone rubber.

1. Thoroughly clean and degrease the surface using a scouring solvent and a slightly abrasive pad on a coarse lint-free cloth. Rinse all cleaning agents off the surface with acetone, MEK or isopropanol. Allow the surface to dry.

2. Alternatively, aqueous degreasing with steam or hot water and appropriate additives can be used to effectively prepare surfaces. Rinse with dematerialized water and allow to dry thoroughly. Ensure that no residues are left on the surface.

3. Apply a thin coat of *Dow Corning* 1200 OS Primer by dipping, brushing or spraying. In most cases, a thin primer film will give best adhesion. Film thickness can be roughly estimated by appearance, the thicker the film the stronger the white tint. If cracks appear in the chalked film, the coat applied was too heavy. In this case, cleaning of the prime coat is recommended, followed by a second application of a thin coat.

Technical Data Sheet

# Sika® Activator

**Technical product data:**

| | |
|---|---|
| Chemical base | solvent-based adhesion promoter |
| Colour | transparent, clear |
| Density (DIN 51757) | 0,71 kg/l approx. |
| Viscosity | 2 mPas |
| Flash point (DIN 51755) | -4°C |
| Application temperature | +5°C to +25°C |
| Drying time (23°C / 50% R.H.) | 10 mins. to 24 h at temperatures over 15°C<br>30 mins. to 24 h at temperatures below 15°C |
| Storage | store in sealed container in a cool dry place |
| Shelf life | 12 months |
| Transport | classified as hazardous substance, Safety Data Sheet is available from Sika on request |

**Description:**
Sika® Activator is a cleansing and activating agent specifically formulated for the treatment of bond faces in direct glazing work prior to application of various Sika® polyurethane adhesives.

**Areas of application:**
Sika® Activator is used to clean and give improved adhesion on glass, ceramic-coated glass, the cut face of old polyurethane adhesive beads, polyurethane-coated window glass and paints.

**Important note:**
Sika® Activator contains solvent, which may dull the surface finish of some freshly applied paints. Preliminary trials should be carried out. If Sika® Activator is accidentally splashed onto adjacent surfaces, wipe off immediately with a clean, dry cloth. Never apply to porous substrates. Sika® Activator may not dry completely on porous surfaces, and this will prevent the adhesive or sealant from curing properly. Where necessary, adjacent porous surfaces should be masked off.

**Method of application:**
Wipe bond faces with a clean lint-free cloth or absorbent paper towel moistened with Sika® Activator.
N.B.: Apply Sika® Activator sparingly, and apply once only. Wipe off any excess with a clean, dry cloth or paper towel. Reseal container tightly after use. Prolonged exposure to atmospheric moisture will cause Sika® Activator to become inactive.
Coverage: 40 g per m² approx.

For information and advice on the safe handling, storage and disposal of chemical products, users should refer to the current Safety Data Sheet containing physical, ecological, toxicological and other safety-related data for the appropriate type of substance.

**Further information:**
Copies of the following publications are available on request:
- Sika Primer Chart
- Safety Data Sheet

**Note:**


Version 02.00

Technical Data Sheet
Version 9 / 20 / 06

# Sika®-Primer 206 G+P & Sika®-Primer 206 Stix

Technical Product Data (typical values)

| | |
|---|---|
| Chemical base | Pigmented solvent-based polyisocyanate solution |
| Color | Black |
| Density (uncured) | 8.8 lb/gal |
| VOC | 4.7 lb/gal |
| VOC content | 612 grams / liter |
| Viscosity | 10 cps |
| Flash point | 25°F (-4°C) |
| Solid content | 40% |
| Application temperature | 40 - 110°F (5- 43°C) |
| Application method | Brush from can. Direct for Stix |
| Coverage | 0.47 oz/ft2 |
| Drying time[1] over 40°F (5°C)<br>below 40°F (5°C)<br>maximum dry time (temperature independent) | 10 min<br>30 min<br>2 h |
| Storage | Store in sealed container in a cool dry place |
| Shelf life (storage between 50 - 77°F (10 - 25°C)) | 9 months in sealed 250 ml bottle<br>13 months in unopened Stix applicator |

[1] Allow additional drying time at cooler temperatures or for porous substrates.

Industry

**Description**

Sika® Primer-206 G+P is a black, moisture-curing liquid primer specifically formulated for the treatment of bond faces in direct glazing work prior to application of Sika® polyurethane direct glazing adhesives and to improve adhesion of other Sika products.
Sika® Primer-206 G+P is manufactured in accordance with ISO 9001 / 14001 quality assurance system and with the responsible care program.

**Areas of Application**

It is used to touch-up pinchweld scratches, and also act as a corrosion inhibitor on metals. May also be used when a frit band is not available on the perimeter of the glass part to provide partial UV protection to the polyurethane. It is also used as a general purpose primer which is used to promote adhesion to

- Glass
- FRP
- ABS
- Plastics
- Aluminum
- Steel
- Paints

**Method of Application**

Surfaces must be clean, dry and free from all traces of grease, oil and dust and of sound quality. Thoroughly remove all loose particles and residues. When using with Sika Aktivator, follow application instructions for both products.

SPECIALITY

Potters Europe
Engineered Glass Materials Division

# Spheriglass® Solid Glass Microspheres – Product Range

High performance functional fillers & extenders offering unique advantages when used in thermoplastic and thermoset systems.

| GRADE | SIEVE SIZE (MICRONS) | % PASSING | SURFACE AREA $m^2/cc$ | MEDIAN DIAMETER (MICRONS) | 90% BEADS BETWEEN MICRONS |
|---|---|---|---|---|---|
| 1221* | 600<br>100 | | NA | NA | |
| 1216* | 1000<br>850<br>425 | 100<br>90 - 100<br>0 – 20 | NA | NA | 425 - 850 |
| 1416* | 710<br>590<br>425 | 100<br>90-100<br>0 – 20 | NA<br>NA | NA<br>NA | 425 – 590 |
| 1619* | 500<br>425<br>250 | 100<br>90 –100<br>0 – 10 | NA | NA | 250 – 425 |
| 1821* | 355<br>300<br>180 | 100<br>90 – 100<br>0 – 10 | NA | NA | 180 – 300 |
| 1922* | 300<br>250<br>150 | 100<br>90 – 100<br>0 – 10 | NA | NA | 150 – 250 |
| 2024 | 250<br>212<br>106 | 100<br>90 – 100<br>0 – 10 | NA | NA | 106 - 212 |
| 2227* | 180<br>150<br>75 | 100<br>90 – 100<br>0 – 10 | NA | NA | 75 – 150 |
| 2429* | 125<br>106<br>53 | 100<br>90 – 100<br>0 – 10 | NA | NA | 53 - 106 |
| 2530 | 106<br>90<br>63<br>45 | 98 – 100<br>90 – 100<br>30 – 60<br>0 – 30 | 0.09 – 0.40 | 56 – 70 | 2.8 – 100 |
| 2000 | 100<br>63<br>45<br>24 | 99.8 – 100<br>83 – 97<br>67 – 88<br>20 – 40 | 0.4 – 0.8 | 27 – 36 | 3 – 80 |
| 3000 | 100<br>63<br>45<br>24 | 100<br>95 – 100<br>85 – 100<br>45 – 75 | 1.05 – 1.75 | 12 – 26 | 0.8 – 70 |
| 5000 | 45<br>24<br>12 | 100<br>99 – 100<br>75 – 97 | 1.75 – 3.30 | 3.5 – 7.0 | 0.5 – 19.3 |

* ANALYSIS ACCORDING TO BS 6088 USING WIRE MESH SIEVES. OTHER GRADES ANALYSED USING LASTER PARTICLE ANALYSIS AND EXCEED BS 6088 REQUIREMENT.

For further information about the superior performances of Spheriglass® Solid Spheres and advice on how best to use them in your application, please contact us:

**POTTERS EUROPE – ENGINEERED GLASS MATERIALS DIVISION**
**Pontefract Road**
**Barnsley**
**South Yorkshire S71 1HJ**
**United Kingdom.**
**Tel. + 44 (0)1226 704516- Fax. +44 (0)1226 207 615**
**E-mail: incsurfy@pottersgroup.com Website: www.pottersgroup.com**



Ref: 3-03-010-1-07

# Appendix F – Numerical and Experimetal Results Graphs

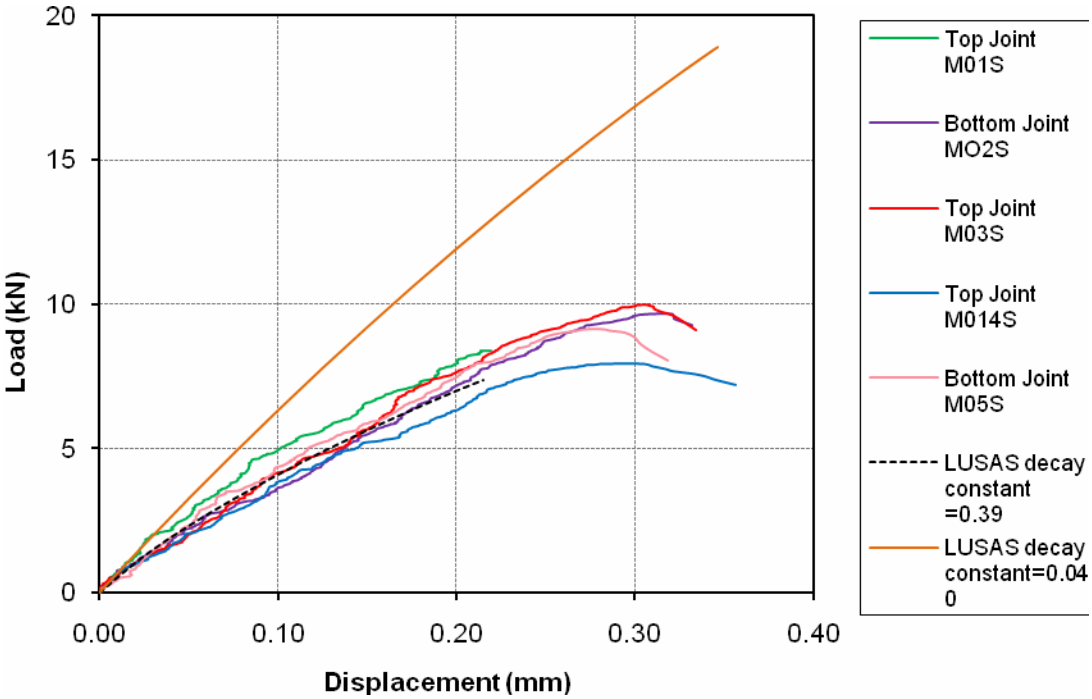


**Graph F13** 3M SLS Numerical and Experimental Results

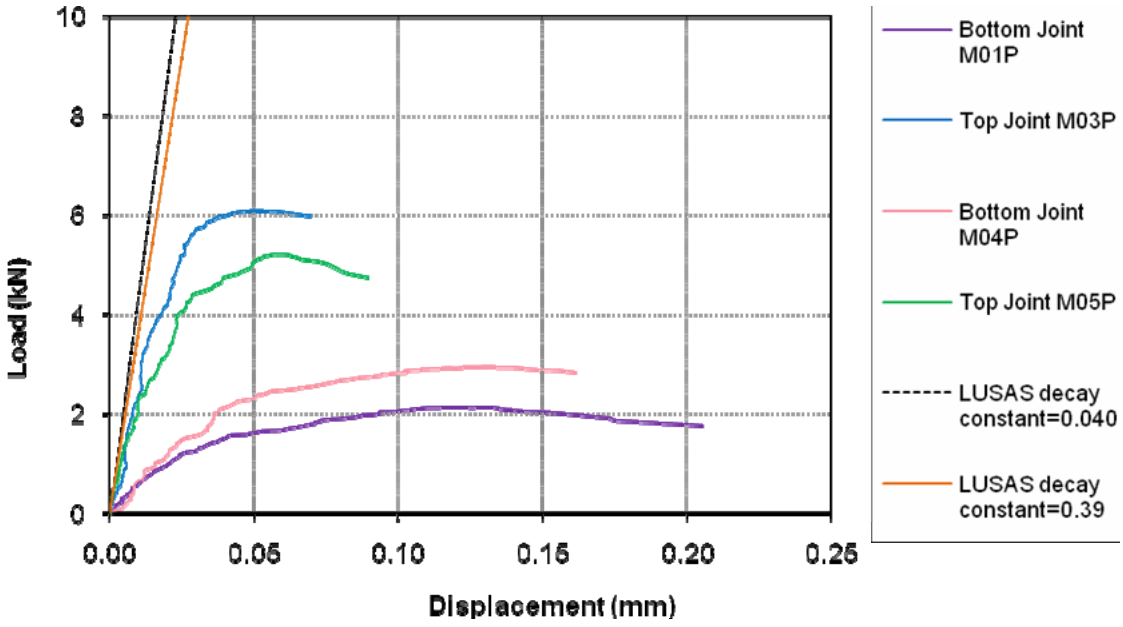


**Graph F2** 3M T-Peel Numerical and Experimental Results

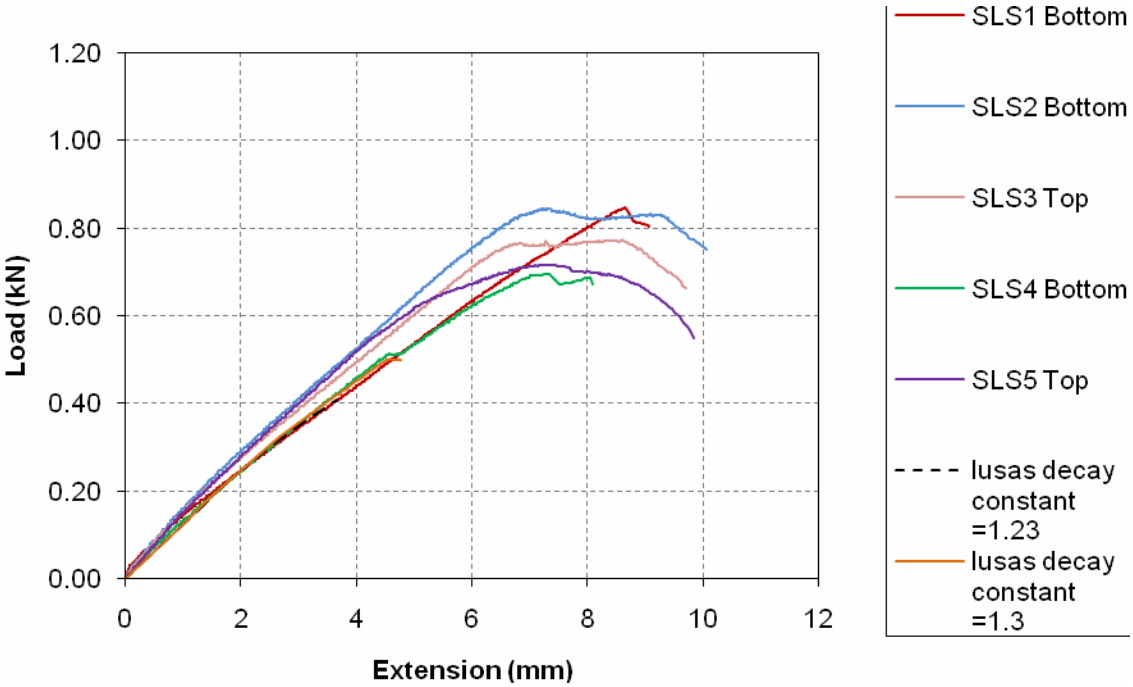


**Graph F3** DC993 SLS Numerical and Experimental Results

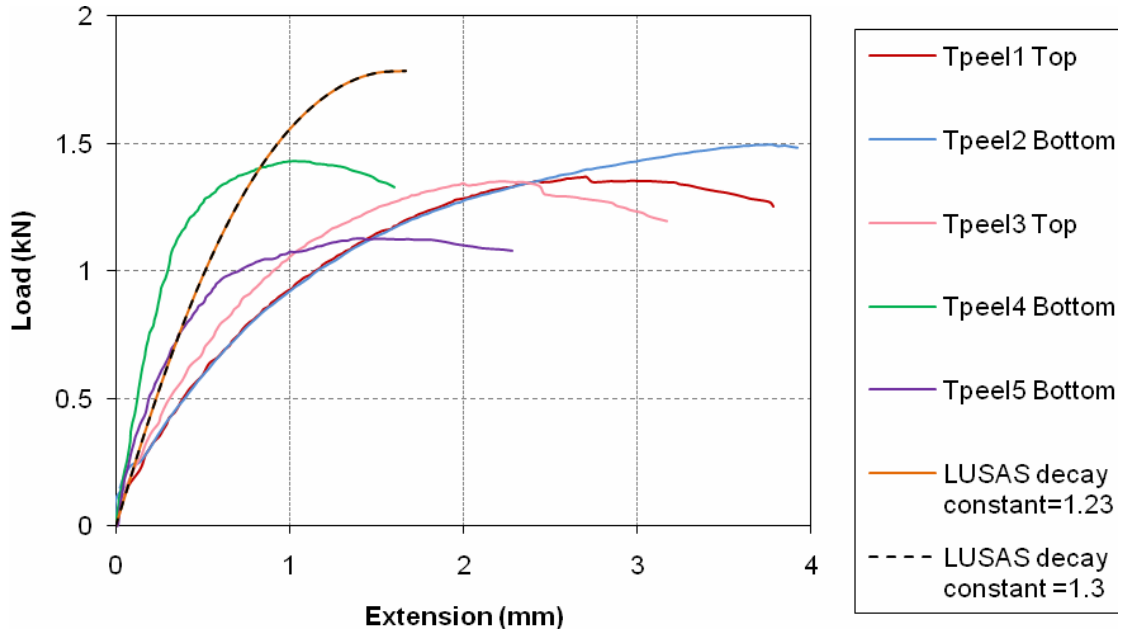


**Graph F4** DC993 T-Peel Numerical and Experimental Results

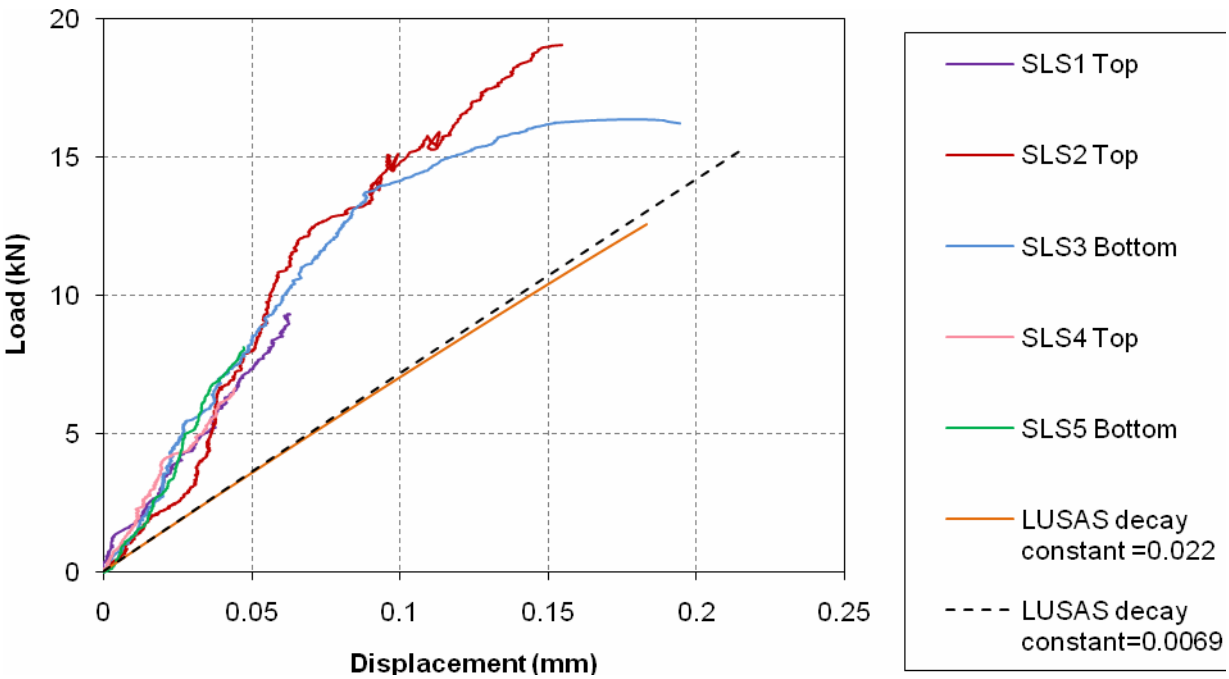


**Graph F5** Bohle SLS Numerical and Experimental Results

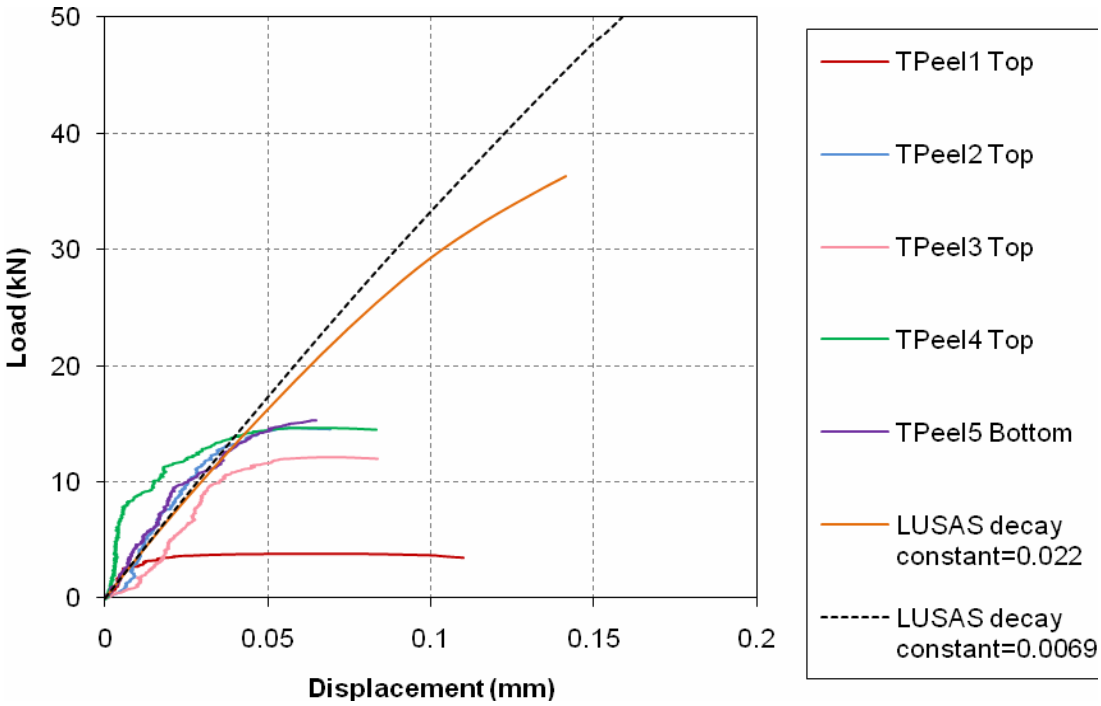


**Graph F6** Bohle T-Peel Numerical and Experimental Results

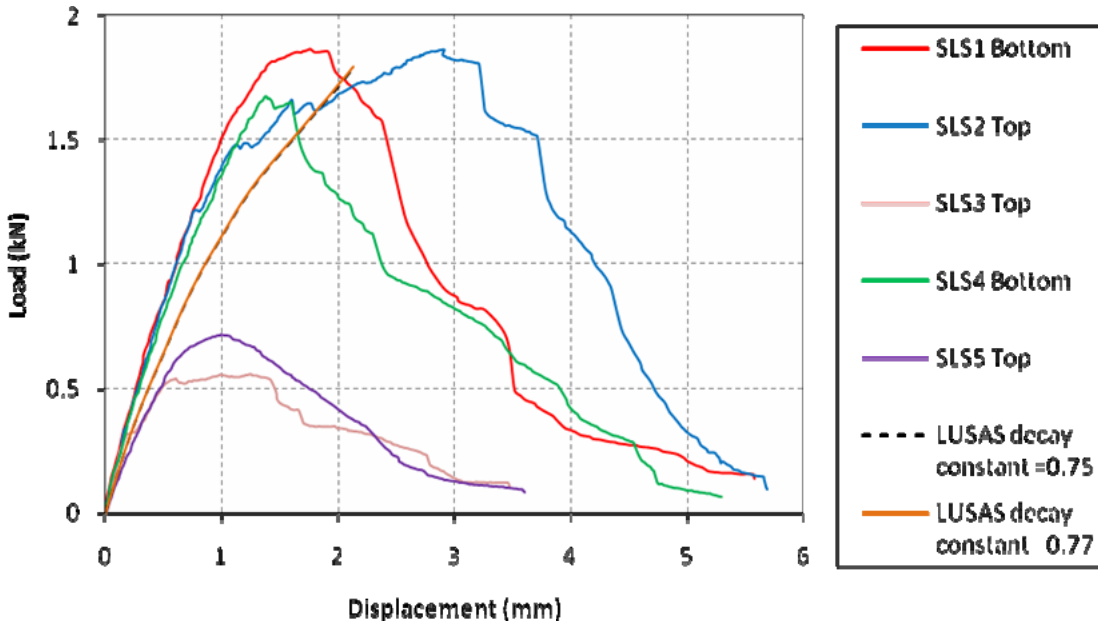


**Graph F7** Sikaforce SLS Numerical and Experimental Results

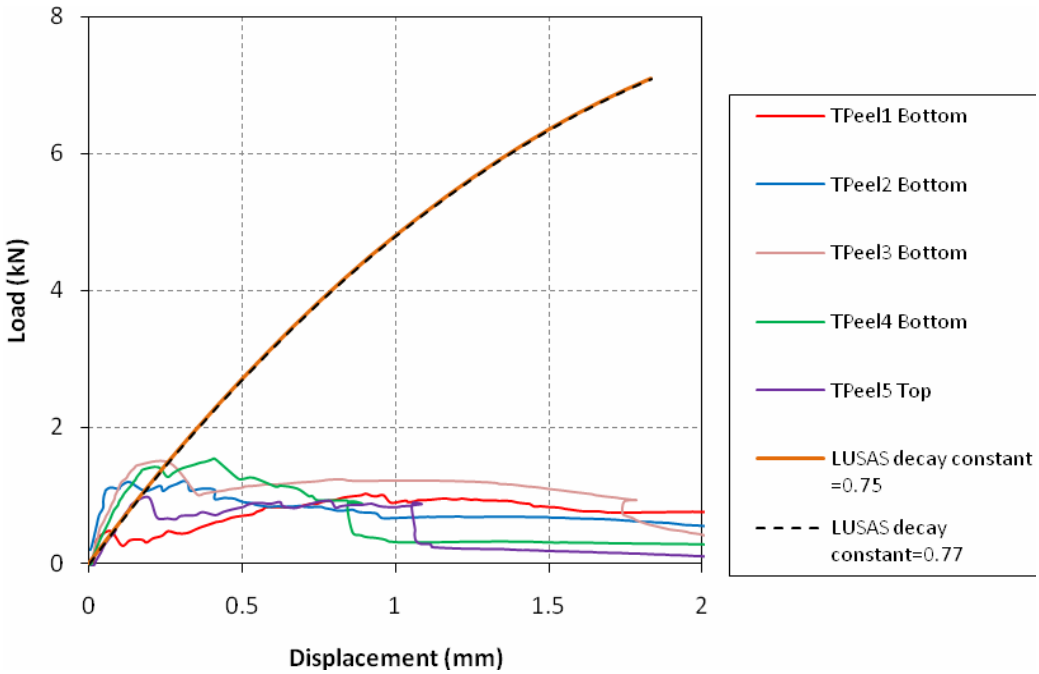


**Graph F8** Sikaforce T-Peel Numerical and Experimental Results

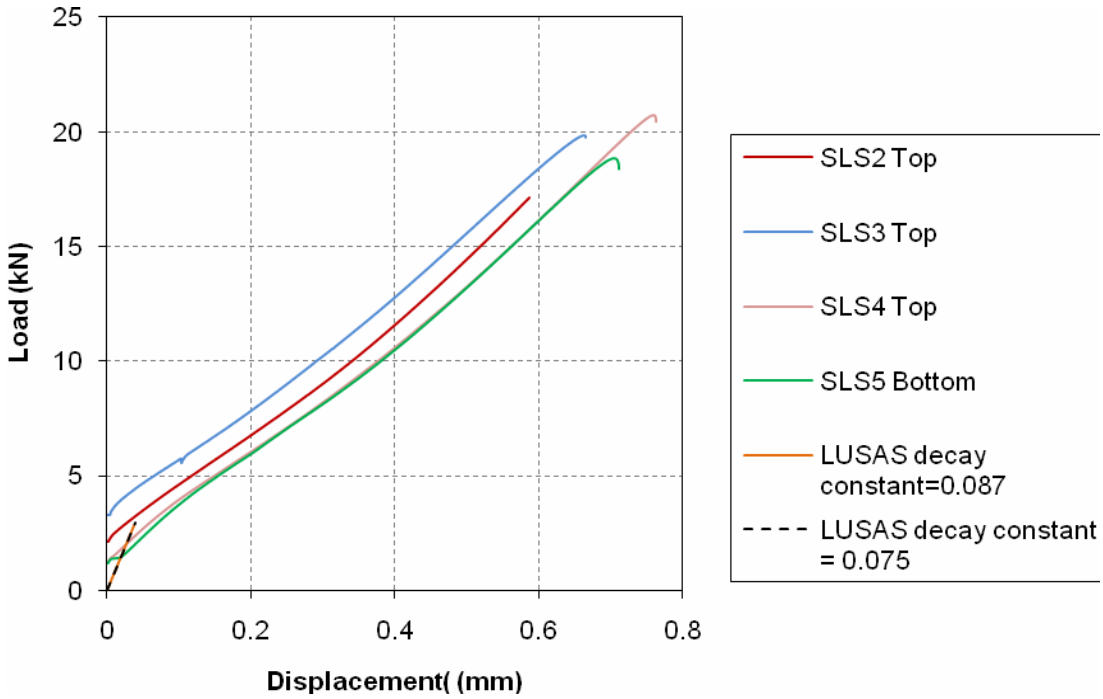


**Graph F9** Holdtite SLS Numerical and Experimental Results

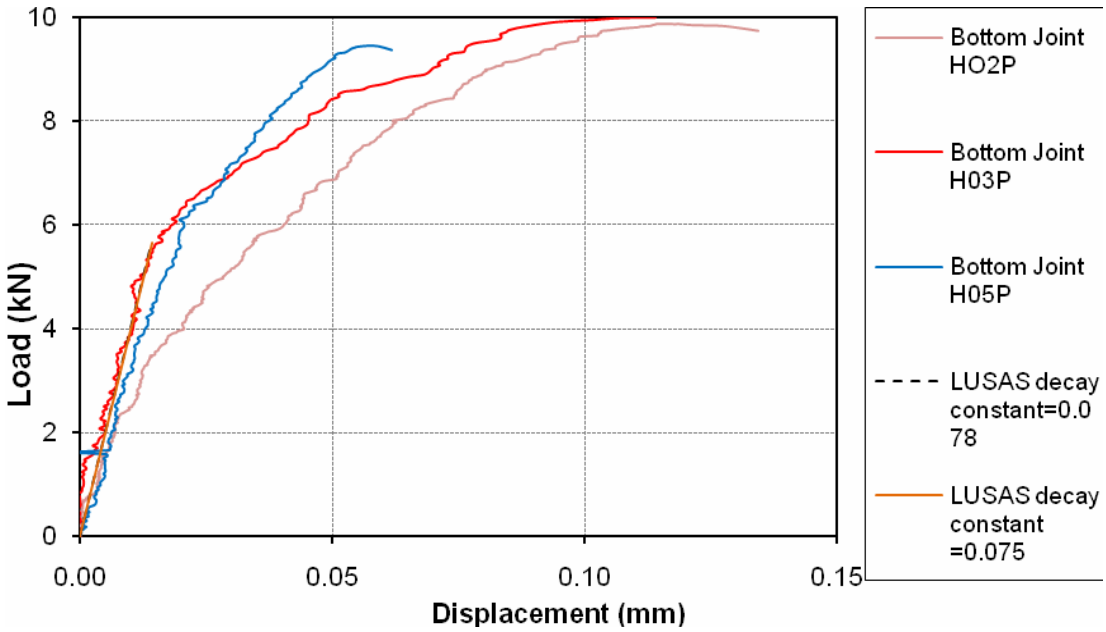


**Graph F10** Holdtite T-Peel Numerical and Experimental Results

# Appendix G – Shear stresses at mid-depth of the 3M SLS joint

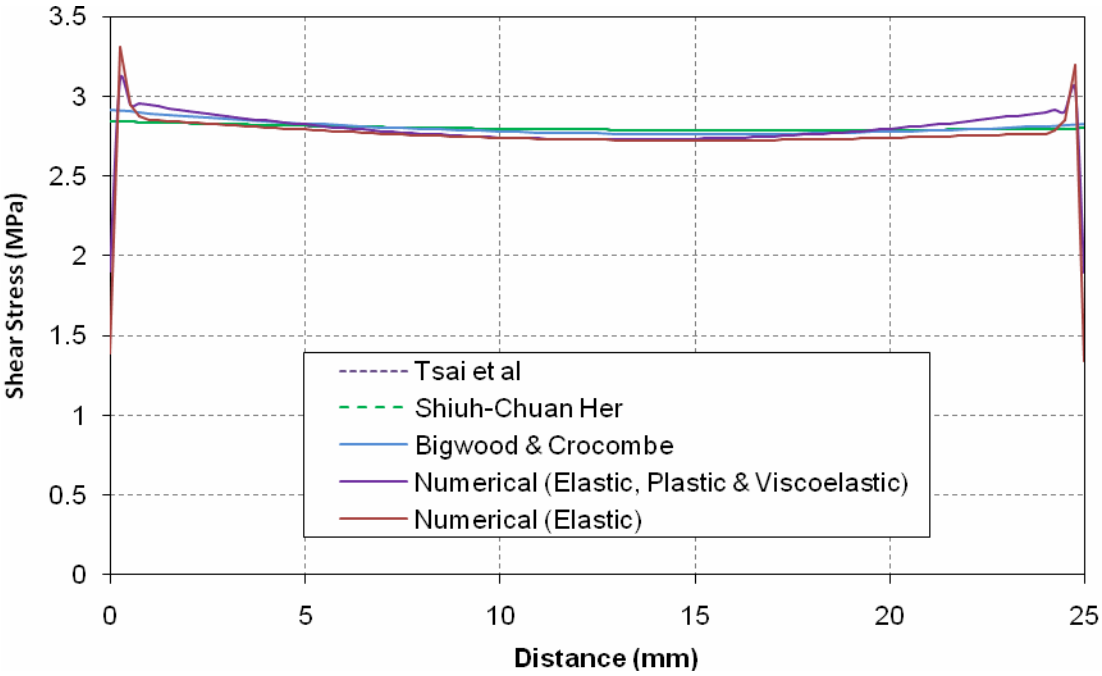


**Graph G1** Analytical and numerical shear stresses at mid-depth of 3M SLS joint ($P$ = 3.5kN)

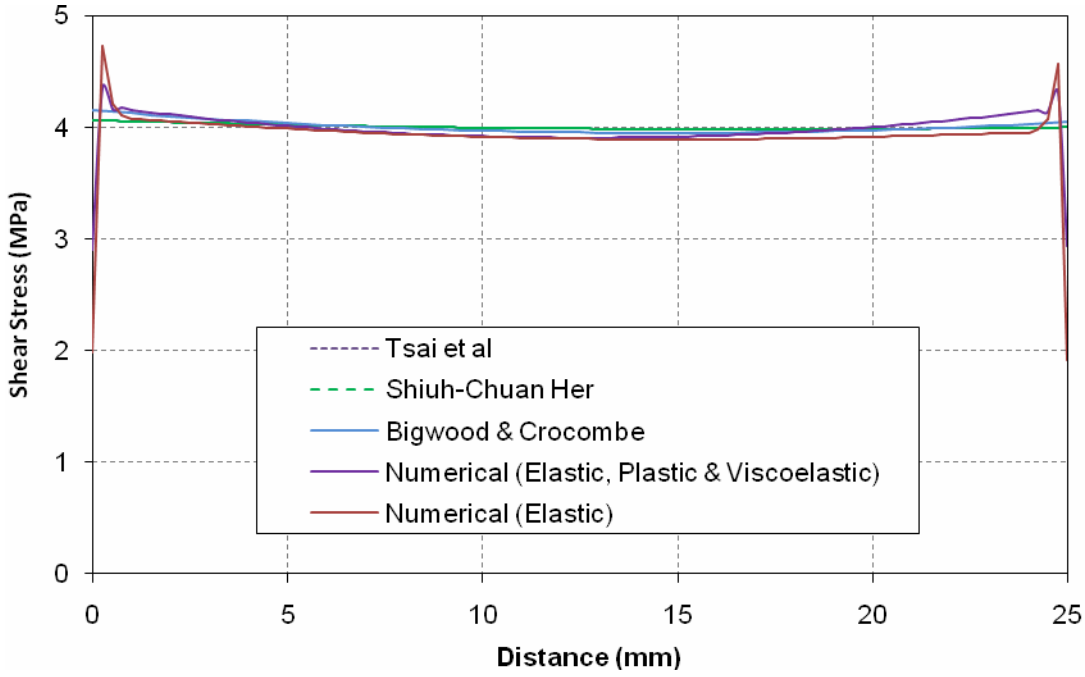


**Graph G2** Analytical and numerical shear stresses at mid-depth of 3M SLS joint ($P$ = 5.0kN)

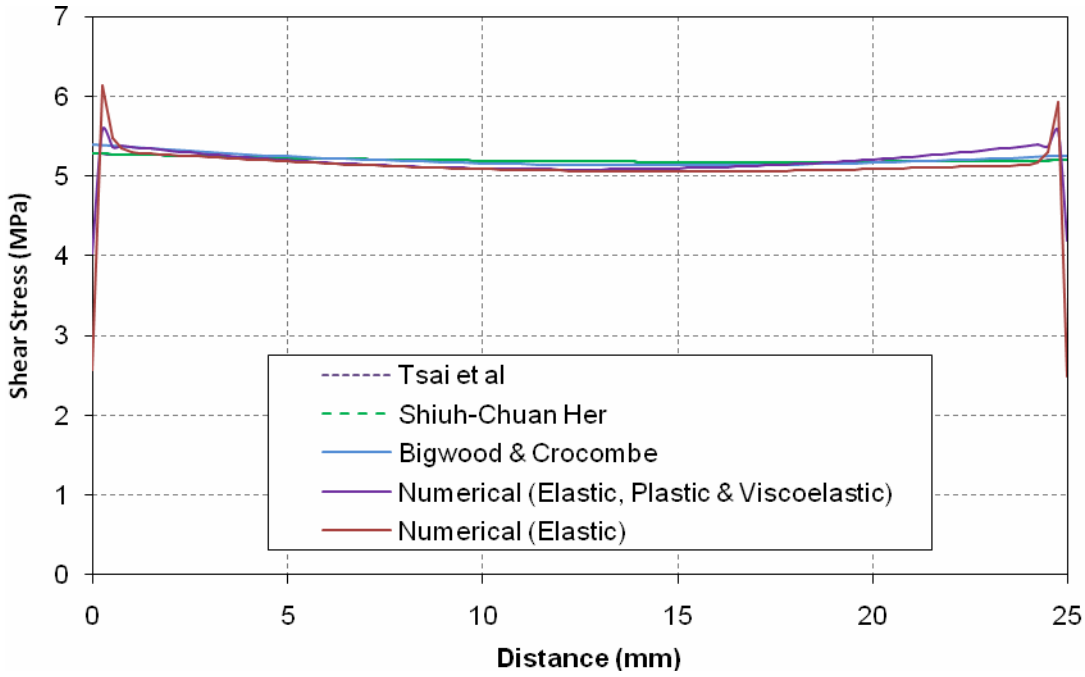


**Graph G3** Analytical and numerical shear stresses at mid-depth of 3M SLS joint ($P$ = 6.5kN)

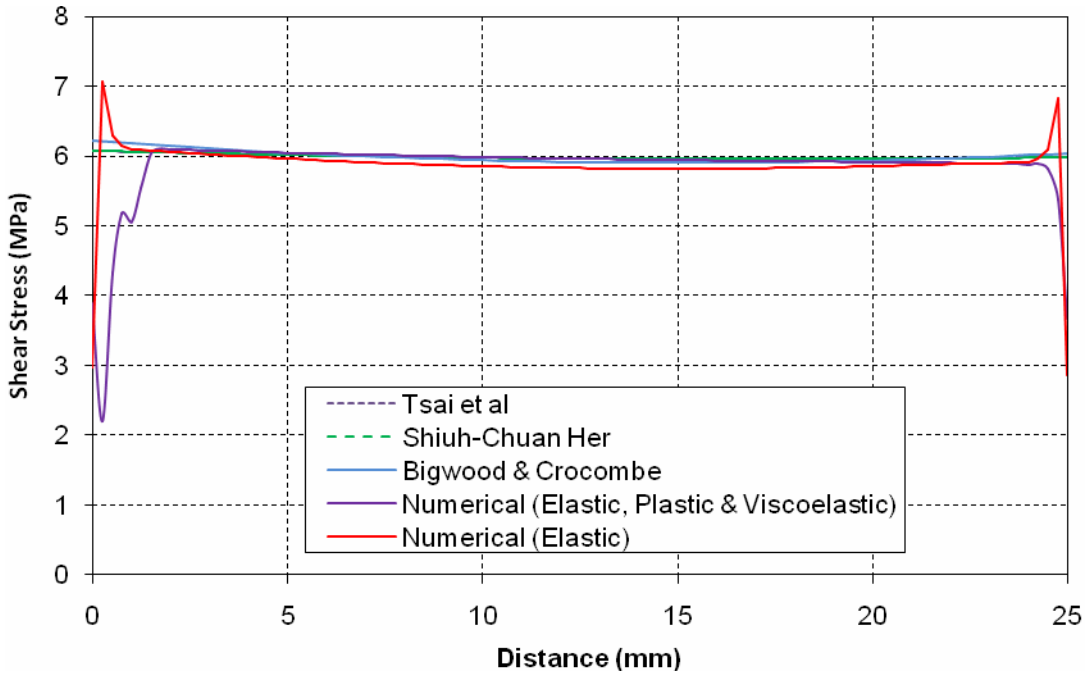


**Graph G4** Analytical and numerical shear stresses at mid-depth of 3M SLS joint at failure load ($P$ = 7.5kN)